

ALPHA PARTICLE MODEL OF ^{16}O

Thesis for the Degree of Ph. D.
MICHIGAN STATE UNIVERSITY

Bing W. Poon

1974



This is to certify that the
thesis entitled

Alpha Particle Model of ^{16}O

presented by

Bing W. Poon

has been accepted towards fulfillment
of the requirements for

Ph. D. degree in Physics

A handwritten signature in cursive script, reading "George Bestak", written over a horizontal line.

Major professor

Date Nov. 5, 1974

69043

ABSTRACT

α Particle Model of ^{16}O

By

Bing W. Poon

The low lying even parity states of ^{16}O are investigated by the coupled-channel method in the weak-coupling model of the α particle and ^{12}C nucleus. Different phenomenological α - α potentials are used in determining the effective α - ^{12}C potential. In calculating the effective α - ^{12}C potential, no intrinsic excited states of ^{12}C are considered, but their effects on different physical properties are calculated. The problem of wave function symmetry is considered. Correct binding energies of the bound states can only be obtained when we use a deep α - α potential. From our results we show that the α - α scattering data do not sufficiently determine the interaction to make predictions on the structure of more complicated nuclei. The interactions with repulsive cores give a very smooth structure to the states and tend to underbind the ground state. Also the transition rates to the 0_2^+ state are too large. The deep attractive interactions suffer from opposite defects. The states are now overbound, and differ

Bing W. Poon

from each other to such an extent that the transition rates are an order of magnitude too small. Of the two types of interaction, we prefer the deep potential, because the structure of the states matches the more fundamental cluster model.

α PARTICLE MODEL OF ^{16}O

By

Bing-W. Poon

A THESIS

Submitted to
Michigan State University
in partial fulfillment of the requirements
for the degree of

DOCTOR OF PHILOSOPHY

Department of Physics

1974

ACKNOWLEDGEMENT

I would like to thank Professor George Bertsch for his guidance and support during the time that this work was performed.

Thanks is also due to Dr. K. Kolltveit for the encouragement and support during the early period of my Ph. D. program, to Professor B. H. Wildenthal for some helpful suggestions.

Lastly, I would like to thank my wife, Viota, without her patience and understanding this work would not have been possible.

TABLE OF CONTENTS

	Page
ACKNOWLEDGEMENTS	ii
LIST OF TABLES	iv
LIST OF FIGURES.	v
INTRODUCTION.	1
 Chapter	
I Historical Review of the α Model	3
II Formalism.	14
Weak Coupling Model Wave Function.	14
Problem of Wave Function Symmetry.	17
Matrix Elements of Electromagnetic Transition Operators	20
Quadrupole Rate with Full Exchange	22
Mean Square Radius with Full Exchange	27
Width of the Resonance	30
III Numerical Details	31
IV Energy Spectra, Wave Functions and Physical Properties.	34
V Summary and Conclusion	43
REFERENCES	45
APPENDIX A	49
APPENDIX B	52

LIST OF TABLES

Table		Page
1	Mixing ratios from TTM's calculation and present calculation.	54
2	Volume integrals of various potentials (V_d being defined in (48)).	55
3	Ground state properties of ^{12}C and ^{16}O from Brink ⁶	56
4	Computation times for the CCE program	56
5a	Mixing ratios of various l in G.S. and 0_2^+ state for Ali and Bodmer potential, also the mixing ratios calculated by Noble and Coelho ³¹	57
5b	Mixing ratios of various l in G.S. and 0_2^+ state for Vary and Dover's folded potential	57
6	Exchange matrix elements	58
7	Ground state binding energies for different potentials	58
8	Excitation energies for different potentials	58
9	Root mean square radii	59
10a	B(E2) transition rates	60
10b	Comparison of our B(E2) and Brown's B(E2) ⁴	61
11	α decay width	61

LIST OF FIGURES

FIGURE		Page
1	Spectra from experiment, TTM's calculation and present calculation using TTM's potential	62
2	Spectra from experiment, calculation using Ali and Bodmer potential and calculation using adjusted Ali and Bodmer potential	63
3	Spectra from experiment, calculation using folded potential and calculation using Neudatchin potential.	64
4	Spectra from experiment and calculation using adjusted folded potential	65
5	Nodes of $\alpha+\alpha$ system in ground state (both particles are located along z axis).	66
6	Nodes of the $\alpha+^{12}\text{C}$ in ground state for Neudatchin potential (the ^{12}C are on the x-y plane)	67
7	Nodes of the $\alpha+^{12}\text{C}$ in 0_2^+ state for Neudatchin potential	68
8	Nodes of the $\alpha+^{12}\text{C}$ in ground state for the adjusted folded potential	69
9	Nodes of the $\alpha+^{12}\text{C}$ in 0_2^+ state for the adjusted folded potential	70
10	The plots of $P_0(\theta)$ for ground state versus $\cos(\theta)$ for different potentials.	71
11	The plots of $P_0(\theta)$ for 0_2^+ state versus $\cos(\theta)$ for different potentials	72
12	Ground state wave function for Ali and Bodmer potential	73
13	0_2^+ state wave function for Ali and Bodmer potential	74

FIGURE		Page
14	Ground state wave function for Folded potential	75
15	0_2^+ state wave function for Folded potential	76

INTRODUCTION

The low lying even parity states of ^{16}O have been difficult to understand in the language of shell model since their energies are much lower than expected on the basis of single particle energies.¹ Also the electromagnetic properties of these states have further emphasized the complex nature of this nucleus. For example, the existence of a rotational band among these states requires strong deformation^{2,3} and the strong E2 transition from the 2^+ state at 6.91 MeV requires states mixing in the ground state. A shell model representation of the 0^+ state of ^{16}O at 6.06 MeV is discussed by Brown and Green⁴ using mainly 4p-4h state. This state has a particular mixture of shell configurations giving a triaxially deformed density distribution. The number of configurations needed to describe this state is very large, and an even greater number would be needed to calculate the energy of the state.⁴⁹ To obtain a wave function usable for discussing the electromagnetic properties, mixing is required between this state, a similar 2p-2h state, and the closed shell state. Bertsch and Bertozzi⁵, using a particle model and making suitable approximations on the wave function of four interacting particles, found the radius of the ground state and the energies of the ground and first 0^+

state agree very well with experimental values. Since the α particle model provides a much more transparent description of the structure of ^{16}O , a more detailed investigation of α particle model on ^{16}O is desired.

We start by assuming the ^{16}O is made up of a ^{12}C core plus an α particle. Since we know the realistic α - α potential and the structure of the ^{12}C ,^{6,7,8} we can calculate the effective α - ^{12}C potential. We put the wavefunction of the system in a weak coupling model form,⁹ use the effective α - ^{12}C potential, and find a set of coupled channel equations from the Schroedinger equation. After we solve these equations, we obtain the spectrum and the wave functions. We use the wave functions to calculate the electromagnetic transition rates and other physical properties of these states.

In Chapter I, we will outline a brief historical review of the α model. In Chapter II, we will show the formalism we needed in our calculation. In Chapter III, we will present the numerical method we used in our calculation. The spectra, wave functions and some physical properties will be shown in Chapter IV. In Chapter V, we will present the summary and conclusion of our calculation.

CHAPTER I

Historical Review of the α Model

The α particle model of the nuclei was first introduced by Gamow in 1930¹⁰ as an extension of his successful investigation of α decay. At that time, nuclei were thought to be composed almost entirely of α particles or protons and electrons. The idea went out of favor when the neutron was discovered and Heisenberg and Majorana had developed their simple and satisfying theories of nuclear structure. However, many physicists felt that the central field approximation needed for the shell model was probably not valid for light nuclei.¹¹ In 1936 this feeling was augmented by Bohr who showed that the binding energies for most nuclei could be reproduced quite well with a liquid drop model.¹² Subsequently the α model was revived in three different forms:

- 1) The first approach was introduced by Margenau¹³ in 1941, and initial investigations were made by Brink¹⁴ and by Biel.¹⁵ In this approach, the wave function of the $4N$ nucleons is

$$\phi_i = A e^{-\frac{(r-R_i)}{2b^i}} \quad i = 1, N$$

where

$$A = \frac{1}{\sqrt{b^3 \pi^{3/2}}}$$

The N vectors R_1 to R_N are parameters representing the center of the N α particles. The wave function ϕ_i describes the motion of a single nucleon in a $1s$ harmonic oscillator orbit centered at the point R_i . A $4-N$ nucleon state may be constructed from these N orbital wave functions by requiring that each orbit state should be occupied by 2 protons and 2 neutrons and then forming the corresponding $4-N$ particle normalized Slater-determinant wave function $\Psi(R_1, \dots, R_N)$. Using the variational principle

$$\delta \left(\frac{\langle \Psi | H | \Psi \rangle}{\langle \Psi | \Psi \rangle} \right) = 0.$$

we can obtain the R_i and b .

Using this approach, Brink, et al.⁶ found the maximum binding for $^{16}_0\text{O}$ when R_i are at the corners of a regular tetrahedron. The value of the binding energy they obtained (Table 1) is 94.4 MeV as compared to the experimental value of 127.6 MeV. They also found that the excitation energies of different α configurations is very sensitive to the nature of the 2-body force. Because the forces they used are not considered realistic enough, they could not get a definite assignment of α configurations to observed levels.

This type of approach requires the center of each α cluster to be fixed, and as a result the Slater determinant states are not eigenstates of angular momentum and often not eigenstates of parity either. Also a recent investigation by Irvine and Abulaffio¹⁶ found an α -cluster configuration is more bound than the optimum regular tetrahedron and there is no sharp minimum in the energy of the ground state of ^{16}O in this model. This suggests that the ground state must be a mixture of α -clusters configurations, or that it is important to treat the cluster coordinates as dynamical variables.

2) A second α -particle model which considers the dynamical motion to some extent was introduced by Wefelmeiser¹⁷ and developed by Wheeler,¹⁸ Dennison,¹⁹ Kameny²⁰ and Perry and Skyrme.²¹ It is assumed that the N α nuclei may be treated as a system of N alpha particles which obey Bose-Einstein statistics (the α particle considered here has no internal structure). This approach actually is the extension of Wheeler's α -cluster model,^{22,23,24,25} the added assumption (α with no internal structure) is to simplify the antisymmetrization of the wave function in Wheeler's α -cluster model.

In this model, the total Hamiltonian is written as

$$H = H_{\text{int}} + H_{\text{rot}}$$

where H_{vib} = vibrational Hamiltonian

H_{rot} = rotational Hamiltonian.

By applying the results of molecular theory to determine the allowed rotational and vibrational quantum states of the nucleus, one can get for ^{16}O :¹⁸

$$E = E_0 + \left(\frac{\hbar^2}{2I}\right)(J(J+1)) + n_1 \hbar \omega_1 + n_2 \hbar \omega_2 + n_3 \hbar \omega_3 + \epsilon$$

where E_0 is the ground state binding energy of the nucleus

I is the moment of inertia of the nucleus

$n_1 \hbar \omega_2$ is the single vibrational energy

$n_2 \hbar \omega_2$ is the doubly degenerate vibrational energy

$n_3 \hbar \omega_3$ is the triply degenerate vibrational energy

ϵ is the vibrational energy that one α going through or going around the other 3α to form a symmetric state.

By choosing suitable parameters, one can get a spectrum that agrees very well with the experimental result. Unfortunately they found for ^{16}O the mean life of the 0_2^+ (6.06 MeV) and 2_1^+ (6.92 MeV) states are 15 to 20 times shorter than the experimental result.²⁰

One may say that because this model has undetermined parameters which are fitted to the data, the validity of the α model is not really put to a test. But how bad it is to represent the particle as a structureless particle?

In a recent research made by Abul-Magd,²⁶ the lower bound to the ground state energy of a system of $N\alpha$ particles interacting via a potential determined by α - α scattering experiments is compared with the energies of nuclei with $2N$ protons and $2N$ neutrons. It is concluded that the $N\alpha$ system can in principle be represented as systems of rigid and structureless α particles. So now the remaining question is how things will happen if we put the realistic α - α potential into the α particle model and treat the α coordinates as dynamical variables.

3) The third α -particle model which not only considers the dynamical motion but also uses a real interaction is a 4-particles problem for $^{16}_0\text{O}$. To solve this, there are three different techniques. The first of these is by Bertsch and Bertozzi.⁵ They approximated the 4-particles wave function of $^{16}_0\text{O}$ to reduce the problem to a one dimensional Schroedinger equation which they can solve. The second technique is by Mendez and Seligman.²⁷ They used the harmonic oscillator wave functions as the basis of the system, and used the method developed for 4 particles harmonic oscillator wave function²⁸ to solve the problem. The third technique is by Terasawa, Tanifuji and Mikoshiba.⁹ They separated the 4 particles into a core ($^{12}_6\text{C}$) plus an α particle. In other words, they simplified the 4-particles problem to a 2-particles problem. Using the weak coupling model wave functions as the basis of the system, they can find the spectrum and the wave functions.

Now let us discuss these three different techniques a little bit further.

a) Bertsch and Bertozzi⁵ approximate the ground state wave function of ^{16}O by

$$\psi_0 = \prod_{ij}^6 \phi(r_{ij})$$

and the first excited state wave function by

$$\psi_1 = \frac{1}{\sqrt{6}} \sum_{ij} \phi'(r_{ij}) \prod_{kl}^5 \phi(r_{kl})$$

The Hamiltonian of the system is

$$H = - \sum_i \frac{\hbar^2}{2M_\alpha} \nabla_i^2 + \sum_6 V(r_{ij})$$

where $V(r_{ij})$ is the interaction between α particles.

In terms of the internal coordinates, the intrinsic Hamiltonian is

$$H_{int} = \sum_{ij}^6 \left(- \frac{\hbar^2}{2M_\alpha} \frac{1}{r_{ij}} \frac{\partial}{\partial r_{ij}} r_{ij}^2 \frac{\partial}{\partial r_{ij}} + V(r_{ij}) \right) \\ - \frac{\hbar^2}{2M_\alpha} \sum_{\substack{adj. \\ side}}^{12} 2 \frac{\vec{r}_{ij} \cdot \vec{r}_{kl}}{r_{ij} r_{kl}} \frac{\partial}{\partial r_{ij}} \frac{\partial}{\partial r_{kl}}$$

They considered the α -configuration of ^{16}O as a tetrahedron composed of 2 triangles lying on a common base with apices

joined by the coordinate r_{ij} and they used the angle θ between the two triangles to describe the tetrahedron. Transforming the r_{ij} in the Hamiltonian to θ and simulating the integrations over r_{ij} by replacing r_{ij} by d —an average separation distance, they found the Hamiltonian for the θ variable becomes

$$H_{red} = H_0 + H'$$

where

$$H_0 = -\frac{\hbar^2}{2M_d} \frac{\partial}{\partial \theta} \frac{1 + \sin^2\left(\frac{\theta}{2}\right)}{\frac{3}{4} d^2} \frac{\partial}{\partial \theta} + V\left(\sqrt{3} d \sin \frac{\theta}{2}\right)$$

$$H' = -\frac{\hbar^2}{2M_d} \sum_{mn} \frac{\sin \frac{\theta}{2} \cos \frac{\theta}{2}}{\frac{3}{4} d} \frac{\partial}{\partial r_{ij}} \frac{\partial}{\partial \theta}$$

$$m n \neq i j$$

By neglecting entirely the coupling of the potential energy with the coordinates and treating the off diagonal matrix elements of the coupling in the second order perturbation theory, they found the effective Hamiltonian for the θ coordinates becomes

$$H_{eff} = H_0 + \sum_{mn} \frac{\langle \phi(r_{mn}) | H' | \phi'(r_{mn}) \rangle^2}{E - E_{\phi'}}$$

They treated $\phi(r_{mn})$ as oscillator functions and got

$$H_{\text{eff}} = -\frac{\hbar^2}{m_\alpha} \frac{\partial}{\partial \theta} \frac{\partial}{\partial \theta} \frac{1}{3d^2(1+\cos^2\frac{\theta}{2})} \frac{\partial}{\partial \theta} + V(\sqrt{3}d \sin\frac{\theta}{2})$$

Using Ali and Bodmer's α - α potential,²⁹ they found that both the interaction energy of the α particles and the root mean radii of ^{16}O agree pretty well with the experimental results except the $\langle G.S | R^2 | 6.06 \rangle$.⁵ They also found the peak of the wave function for the ground state is at the regular tetrahedron shape and the excited 0^+ state (6.06 MeV) has a peak at the shape of a plane diamond.

b) Mendez and Seligman²⁷ also did a similar calculation on ^{12}C and ^{16}O . They used harmonic oscillator wave function as the basis of the system and the Hamiltonian is given by

$$H = H_0 + H_1$$

where

$$H_0 = \sum_{i=1}^n \frac{p_i^2}{2m_\alpha} + \frac{m_\alpha \omega^2}{2} \sum_{i < j=1}^n r_{ij}^2$$

$$H_1 = \sum_{i < j=1}^n V_{ij} - \frac{m_\alpha \omega^2}{2} \sum_{i < j=1}^n r_{ij}^2$$

n is the total number of α .

Using some phenomenological α - α potentials for V_{ij} (later they found the best results were those given by Ali and

Bodmer potential) and applying the variational method on the harmonic oscillator parameter $\epsilon = \frac{\hbar\omega}{m_0 c^2}$ (m_0 is the mass of e^-), they found the form factors and the spacing of the 0^+ states for ^{12}C and ^{16}O are reasonable. However, in both cases the ground state binding energies are smaller than the experimental results by a factor of three. They concluded that the α - α potential determined by phase shift method is not strong enough to give the right binding. We will come back to this argument later in Chapter IV.

c) An α -model calculation on ^{16}O which was similar to the one given by Noble and Coelho^{30,31} was done by Terasawa, Tanifuji and Mikoshiba⁹ (later we will refer to them as TTM). They treated the ^{16}O as a system of a ^{12}C core plus an α particle. They used the weak coupling model wave functions as the basis of the system. Putting it into the Schroedinger equation, they obtained a set of coupled channel equations. By solving the equations, they found the spectrum and the wave function. Because our calculation follows closely this approach, we will describe it in more detail in the coming chapters. In their calculation, instead of using a realistic potential, they used a Woods-Saxon potential with undetermined parameters. By choosing the right parameters, they apparently obtained a spectrum in agreement with experiment (Figure 2). In their paper, it is not clear to us what is the Coulomb radius they used in their calculation. So in duplicating their calculation, we use the R_c value

(1.3 fm) used by Tatscheff and Brissand³² whose potential we believe is the original form of TTM's potential. In doing so, we found they used a slightly larger value of R_c (1.75 fm). In Figure 2, we also show our result which is supposed to be identical to TTM's. Although the spectrum we found here does not agree completely with their results, by looking at the mixing ratio of the configurations (Table 1) and the number of nodes for each wave function, we believe these states are exactly those they got. By looking at the wave functions, we found that they all peaked at a very large radius (e.g. the bound 0_2^+ state peaked at about 6 fm), which we believe is not realistic. The reason why the wave functions behave like this can easily be understood if we look at the potential carefully. First of all, this type of potential was first used in the α scattering problem at very high energy (e.g. in Tatscheff and Brissand's paper, they calculated α scattering at $E=166$ MeV), so the radius of potential can be very large and the amplitude of the potential can be very weak. But in calculating the bound states or those states close to a bound state, this type of potential certainly will not give a satisfactory result. Also we know that in considering the exclusion effect, the potential should either have a short range repulsive part²⁹ or have a strong attractive core.³³ But none of these appear in TTM's potential. In Tatscheff and Brissand's paper, the amplitude of the potential was chosen to be $V=100.9$ MeV

compared to $V=62.5$ MeV used by TTM. We believe if we use a larger value of V , the O_2^+ state in TTM's calculation will become the ground state and so the 2^+ states they got will become spurious. Also we believe a lot of states they got will violate the Bose-Einstein statistics which the α particles must obey and should be spurious. We will discuss this in more detail in the next chapter.

In the literature, two similar but stronger potentials were suggested by Neudatchin³³ and by Vary and Dover.³⁴ The results of these potentials will be shown in later chapters. One more remark is that since the wave functions in TTM's calculation are peaked at the outside region, the spectrum depends very much on the cut off radius (R_{\max}) we choose for the wave function unless the R_{\max} is very large. In our calculation here, we put $R_{\max}=10$ fm; that may be the reason why the spectrum is slightly different from TTM's result.

CHAPTER II

Formalism

Weak Coupling Model Wave Function

In our calculation we treat the ^{16}O as a ^{12}C core plus an α particle. The Hamiltonian for the $\alpha + ^{12}\text{C}$ system is given by

$$H = H_t + T + V_{\alpha-^{12}\text{C}}$$

where H_t is the Hamiltonian for the ^{12}C

T is the kinetic energy of the α particle

$V_{\alpha-^{12}\text{C}}$ is the effective potential between the α and the ^{12}C .

The Schroedinger equation can then be written as

$$H \Psi_{JM} = E \Psi_{JM}$$

where Ψ_{JM} is the total wave function of our system in J state.

Let us use the weak coupling model wave function⁹ as our basis, so the total wave function can be written as

$$\Psi_{JM} = \sum_{L_n I_n} \frac{R_{L_n I_n}^J}{\gamma} (Y_{L_n} \otimes \Phi_{I_n})_{JM} \quad (1)$$

where Y_{L_n} is the spherical harmonic function representing the angular part of the α particle in the L_n state

Φ_{I_n} is the internal wave function of the core in the I_n state and satisfies

with ω_n being the excitation energy of the ^{12}C in the n^{th} state. $H_t \Phi_{I_n} = \omega_n \Phi_{I_n}$

Thus the center of mass energy of the α particles which leaves the core in its n^{th} state is given by

$$E_n = E - \omega_n$$

Putting our wave function into the Schroedinger equation, multiplying both sides by $(Y_{L_n} \otimes \Phi_{I_n})_{JM}$ and integrating over all coordinates except the r , we obtain

$$\left[\frac{\hbar^2}{2\mu} \left(\frac{d^2}{dr^2} - \frac{L_n(L_n+1)}{r^2} \right) + E_n \right] R_{L_n I_n}^J(r) = \sum_{L'_n I'_n} \langle (L_n, I_n)_{JM} | V_{\alpha-^{12}\text{C}} | (L'_n, I'_n)_{JM} \rangle \times R_{L'_n I'_n}^J(r) \quad (2)$$

where

$$(L_n, I_n)_{JM} \equiv (L_n \otimes \Phi_{I_n})_{JM}$$

μ is the reduced mass of our system.

The effective potential $V_{\alpha-^{12}\text{C}}$ can be defined to be³⁵

$$V_{\alpha-^{12}\text{C}} = \int f(\Omega) V_{\alpha-\alpha}' d\Omega$$

where $\rho(r)$ is the α density function of the ^{12}C

$$V'_{\alpha-\alpha} = V_{\alpha-\alpha} + V_{\text{coul}}$$

$V_{\alpha-\alpha}$ is the phenomenological α - α potential

V_{coul} is the Coulomb potential between the two α .

Now let us expand the potential in spherical harmonics

$$V_{\alpha-^{12}\text{C}} = \sum_{l m} V_l^m(r) Y_l^m(\theta', \phi') \quad (3)$$

$$= \sum_{l m k} V_l^m(r) D_{kM}^l(\theta_i, \phi_i) Y_{l k}(\theta, \phi)$$

where

$$V_l^m(r) = \int V_{\alpha-^{12}\text{C}} Y_l^m(\theta', \phi') d\Omega' \quad (4)$$

θ', ϕ' refer to the body fixed system

θ, ϕ refer to the α coordinates in the space fixed system

θ_i, ϕ_i refer to the Euler angles between the body fixed and the space fixed systems.

Equation (2) can be rewritten as (Appendix A)

$$\left[\frac{\hbar^2}{2\mu} \left(\frac{d^2}{dr^2} - \frac{L_n(L_n+1)}{r^2} \right) + E_n \right] R_{L_n I_n}^J(r)$$

$$= \sum_{L'_n I'_n} \sum_{\ell m K'} V_\ell^m(r) A(L_n I_n L'_n I'_n \ell m K' K J) \int_{K'+m, K}^J R_{L'_n I'_n}^J(r) \quad (5)$$

$$A(L_n I_n L'_n I'_n \ell m K' K J) = (-1)^{J+\ell+m+L_n+L'_n+I_n} \sqrt{\frac{(\ell+L_n+1)(\ell+L'_n+1)(\ell+I_n+1)}{4\pi(\ell+1)(\ell+1)}}$$

$$\times (L_n L'_n 0 0 | \ell 0) (I'_n \ell K' m | I_n K) U(L_n I_n L'_n I'_n; J \ell) \quad (5a)$$

where $U(LI, L'I'; J\ell)$ is the Racah U-coefficient

$(J_1 J_2 M_1 M_2 | JM)$ is the Clebsch Gordon coefficient

Solving these coupled channel equations, we can find the energy E_n and the wave function.

Problem of Wave Function Symmetry

The alphaparticles must obey Bose-Einstein statistics. In an exact α theory, the Hamiltonian would be symmetric with respect to α coordinates, and the wave functions would have definite symmetries, so all that would be necessary would be to select out the totally symmetric states. This is obvious in the 2α problem, where all that is necessary is to throw out the odd parity solutions. In our model with $\alpha + {}^{12}\text{C}$, symmetries are no longer evident and there will be

extra states that are not obviously spurious. However, we can construct a model for the ^{12}C as $\alpha + {}^8\text{Be}$, and calculate the matrix element of the α exchange operator. Ideally, this matrix element would be +1 for the true states, and all other states could be rejected. The details of the construction of this operator are as follows.

Let us define the exchange matrix elements as

$$E_C^J = \langle \Psi_J(\alpha_1 \leftrightarrow \alpha_2 + \alpha_3 + \alpha_4) | P_{12} | \Psi_J(\alpha_1 \leftrightarrow \alpha_2 + \alpha_3 + \alpha_4) \rangle$$

Here the notation $\Psi_J(\alpha_1 \leftrightarrow \alpha_2 + \alpha_3 + \alpha_4)$ means the wave function of the number 1 α particle moving relative to the core which made up of the three α particles α_2 , α_3 and α_4 . P_{12} is the exchange operator exchanging α_1 and α_2 . Now let us decouple the core into one α moving around a small core (${}^8\text{Be}$), so the wave function becomes

$$\begin{aligned} \Psi_J(\alpha_1 \leftrightarrow \alpha_2 + \alpha_3 + \alpha_4) &= | \Psi_J(\alpha_1 \leftrightarrow \alpha_2 + {}^8\text{Be}) \rangle \\ &= \sum_{l_n I_n} \frac{R_{l_n I_n}(r_1)}{r_1} \left\{ \gamma_{l_n}(\alpha_1) \otimes \Phi_{I_n}(\alpha_2 + {}^8\text{Be}) \right\}_J \\ &= \sum_{l_n I_n} \frac{R_{l_n I_n}(r_1)}{r_1} \left\{ \gamma_{l_n}(\alpha_1) \otimes \left[\sum_{j_1, j_2} \frac{u_{j_1, j_2}(r_2)}{r_2} (\gamma_{j_1}(\alpha_2) \otimes \chi_{j_2}({}^8\text{Be})) \right]_{I_n} \right\}_J \\ &= \sum_{\substack{l_n I_n \\ j_1, j_2}} \frac{R_{l_n I_n}(r_1)}{r_1} \frac{u_{j_1, j_2}(r_2)}{r_2} \left\{ \gamma_{l_n}(\alpha_1) \otimes \left[\gamma_{j_1}(\alpha_2) \otimes \chi_{j_2}({}^8\text{Be}) \right]_{I_n} \right\}_J \end{aligned}$$

where r_1 is the distance between the C.M. of ^{12}C and the α_2

r_2 is the distance between the C.M. of ^8Be and the α_2 in ^{12}C system.

Here $R_{L_n I_n}(r_1)$ represents the radial part of the wave function when α_1 is moving around the core ^{12}C , and $U_{I_1 I_2}(r_2)$ represents the radial part of the wave function when α_2 is moving around the core ^8Be . We can then express the wave function with particle 1 and particle 2 interchanged as

$$P_{12} |\Psi_J(\alpha_1 \leftrightarrow \alpha_2 + ^8\text{Be})\rangle = |\Psi_J(\alpha_2 \leftrightarrow \alpha_1 + ^8\text{Be})\rangle$$

$$= \sum_{\substack{L'_n I'_n \\ I'_1 I'_2}} \frac{R_{L'_n I'_n}(r_2)}{r_2} \frac{U_{I'_1 I'_2}(r_1)}{r_1} \left\{ \gamma_{L'_n}(\alpha_2) \otimes \left[\gamma_{I'_1}(\alpha_1) \otimes \gamma_{I'_2}(^8\text{Be}) \right]_{I'_n} \right\}_J$$

Using the Racah Coefficient,³⁶ we can recouple this wave function into

$$P_{12} |\Psi_J(\alpha_1 \leftrightarrow \alpha_2 + ^8\text{Be})\rangle$$

$$= \sum_{\substack{L'_n I'_n \\ I'_1 I'_2}} \frac{R_{L'_n I'_n}(r_2)}{r_2} \frac{U_{I'_1 I'_2}(r_1)}{r_1} \sum_{\mathcal{L}} U(L'_n I'_1, J I'_2; \mathcal{L} I'_n)$$

$$\times \left[\gamma_{I'_1}(\alpha_1) \otimes (\gamma_{L'_n}(\alpha_2) \otimes \gamma_{I'_2}(^8\text{Be}))_{\mathcal{L}} \right]_J$$

Now we can evaluate the overlap of this wave function with a wave function in our standard representation by neglecting the difference between the CM of the ${}^8\text{Be}$ and ${}^{12}\text{C}$

$$\begin{aligned}
 EC^J &= \langle \Psi_J(\alpha_1 \leftrightarrow \alpha_2 + {}^8\text{Be}) | P_{12} | \Psi_J(\alpha_1 \leftrightarrow \alpha_2 + {}^8\text{Be}) \rangle \\
 &= \sum_{\substack{L_n=L'_n \\ I_n=I'_n \\ I_1=I'_1 \\ I_2=I'_2}} \sum_{\substack{L'_n L'_1 \\ L'_n I'_1}} \int R_{L'_n I'_n}(r_2) U_{L'_n I'_n}(r_2) dr_2 \int R_{L_n I_n}(r_1) U_{L_n I_n}(r_1) dr_1 \\
 &\quad \times U(L'_n I'_1, J I'_2; L_n I'_n)
 \end{aligned}$$

To obtain this result, we require

$$\langle Y_{L_n}(\alpha_1) \otimes \phi_{I_n}^{\text{ang}}(\alpha_2 + {}^8\text{Be}) | Y_{L'_n}(\alpha_1) \otimes \phi_{I'_n}^{\text{ang}}(\alpha_2 + {}^8\text{Be}) \rangle = \delta_{L_n L'_n} \delta_{I_n I'_n}$$

where $\phi_{I_n}^{\text{ang}}(\alpha_2 + {}^8\text{Be})$ is the angular part of the core's wave function with angular momentum equal to I_n .

By inspecting the exchange matrix element, we can find the symmetric states of our system. We will come back to this problem in Chapter IV.

Matrix Elements of Electromagnetic Transition Operators

To find the electric transition rate, we start with the equation³⁷

$$B(E1, L) = \left[\frac{1}{\sqrt{(2J_i+1)}} (\Psi_j \| \frac{1}{e} \sum_{j=1}^n e_j r_j^L Y_{LM}(\theta_j, \phi_j) \| \Psi_i) \right]^2$$

where n is the total number of α particles in the nuclei
in our case $n = 4$

e_j is the charge of the α particle (i.e. $e_j = 2e$).

Now let us separate the right hand side into two terms

$$B(E_L, L) = [Q_\alpha + Q_{12C}]^2$$

where

$$Q_\alpha = \frac{1}{\sqrt{(2J_i+1)}} (\Psi_f \parallel 2r_i^L Y_L(\theta_i, \phi_i) \parallel \Psi_i)$$

and

$$Q_{12C} = \frac{1}{\sqrt{(2J_i+1)}} (\Psi_f \parallel 2 \sum_{j=2}^4 r_j^L Y_L(\theta_j, \phi_j) \parallel \Psi_i)$$

Physically we can say the Q_{12C} comes from the three α particles in the core, and Q_α comes from the extra α particle.

Using our form of the wave function (Eqn. 1), we can get (Appendix B)

$$Q_\alpha = \sum_{l_n l'_n l_n} 2 \left[\int_0^\infty R_{l_n l'_n}^{J_f^*}(r) r^L R_{l'_n l_n}^{J_i}(r) dr \right] (-1)^{l_n + l'_n + J_f}$$

$$\times \sqrt{\frac{(2J_f+1)(2l_n+1)}{4\pi(2l_n+1)}} U(l_n l'_n J_f J_i; L l_n) (l'_n l_n 0 0 | l_n 0)$$

$$Q_{n_c} = \sum_{L_n' I_n'} (-1)^{L_n' + L + I_n + J_i} \sqrt{\frac{(2L_n+1)(2J_f+1)}{(2L+1)(2L_n'+1)}} U(L_n L_n' J_f J_i; L L_n')$$

$$\times \left[\int R_{L_n' L_n}^{J_f*}(r) R_{L_n' I_n'}^{J_i}(r) dr \right] Q_{n_c}(L_n' \rightarrow I_n)$$

where $[Q_{12_C}(I_n' \rightarrow I_n)]^2$ is the electric transition rate between the states I_n' and I_n of the core ^{12}C . In our calculation, we use the experimental values and the values predicted by the rotor model as our values of $[Q_{12_C}(I_n' \rightarrow I_n)]^2$.

Quadrupole Rate with Full Exchange

As we mentioned before, ideally the exchange matrix elements would be +1 for the true states, but in our calculation we found all of them are very much smaller than +1 except the one for the ground state; the reason for this is presumably because of the inadequacy of basis: no intrinsic excited states of ^{12}C are being considered. Because the exchange matrix elements are smaller than one, we no longer can rely on the formula mentioned in the previous section in calculating the quadrupole rate (Eqn. (6) and Eqn. (6.a)). A better approximation for the wave function is

$$\begin{aligned}
 |\Psi_{J'}\rangle &= N^{J'} (1 + P_{12} + P_{13} + P_{14}) \sum_{L'_n I'_n} \frac{R_{L'_n I'_n}(r_1)}{r_1} \frac{U_{J' I'_n}(r_1)}{r_2} |Y_{L'_n}^{(1)} \otimes (Y_{I'_n}^{(2)} \otimes Y_{I'_n}^{(3)})\rangle_J \\
 &\equiv N^{J'} (1 + P_{12} + P_{13} + P_{14}) |\Phi^{J'}\rangle
 \end{aligned}$$

where $N^{J'}$ can be written as $N^{J'} = (4 + 12 \times EC^{J'})^{-\frac{1}{2}}$

From Appendix B we can find

$$\begin{aligned}
 \langle \Phi^J | r_1^l Y_l^m(\alpha_1) P_{12} | \Phi^{J'} \rangle &= \sum_{\substack{L_n I_n \\ I'_1 I'_2}} \sum_{\substack{L'_n I'_n \\ I'_1 I'_2}} \sum_{\substack{M_n M_{I_n} \\ M_{I'_1} M_{I'_2}}} \left[\int R_{L_n I_n}(r_1) U_{I'_1 I'_2}(r_1) r_1^l dr_1 \right] \\
 &\times \left[\int U_{I_1 I_2}(r_2) R_{L'_n I'_n}(r_2) dr_2 \right] (L_n M_n L_n M_{I_n} | J M) (I'_1 M_{I'_1} I_n M_{I_n} | J' M') \\
 &\times U(L'_n I'_1, J' I'_2; I_n I_n) \langle Y_{L_n}^{M_n}(\alpha_1) | Y_{L_n}^M(\alpha_1) | Y_{I'_1}^{M_{I'_1}}(\alpha_1) \rangle
 \end{aligned}$$

and

$$\begin{aligned}
 \frac{1}{\sqrt{(2J'+1)}} (\Phi^J || r_1^l Y_l^m || P_{12} \Phi^{J'}) &= \sum_{\substack{L_n I_n \\ I_1 I_2}} \sum_{\substack{L'_n I'_n \\ I'_1 I'_2}} \left[\int R_{L_n I_n}(r_1) U_{I'_1 I'_2}(r_1) r_1^l dr_1 \right] \\
 &\times \left[\int U_{I_1 I_2}(r_2) R_{L'_n I'_n}(r_2) dr_2 \right] (-1)^{J'+L_n+l+L'_n} \sqrt{\frac{(2J'+1)(2L_n+1)}{4\pi(2L_n+1)^2}} \\
 &\times U(L_n I_1, J J'; l L_n) U(L'_n I'_1, J' I'_2; I_n I_n) \\
 &\times (L_n l 0 0 | I_1 0) \delta_{I_2 I'_2} \delta_{I_1 L'_1}
 \end{aligned}$$

To evaluate the quadrupole rate with full exchange, first we have to determine

$$\begin{aligned}
& (\phi^J (1 + P_{12} + P_{13} + P_{14})^\dagger \parallel r_1^2 \gamma_2(\alpha_1) \parallel (1 + P_{12} + P_{13} + P_{14}) \phi^{J'}) \\
& \simeq (N^J N^{J'}) \left[(\phi^J \parallel r_1^2 \gamma_2(\alpha_1) \parallel \phi^{J'}) + \sum_{i=2}^4 (\phi^J \parallel r_i^2 \gamma_2(\alpha_i) \parallel \phi^{J'}) \right. \\
& + (\phi^J \parallel r_1^2 \gamma_2(\alpha_1) (P_{12} + P_{13} + P_{14}) \parallel \phi^{J'}) + (\phi^J \parallel (P_{12} + P_{13} + P_{14})^\dagger r_1^2 \gamma_2(\alpha_1) \parallel \phi^{J'}) \\
& + (\phi^J \parallel \{ P_{12}, r_3^2 \gamma_2(\alpha_3) \} \parallel \phi^{J'}) + (\phi^J \parallel \{ P_{12}, r_2^2 \gamma_2(\alpha_2) \} \parallel \phi^{J'}) \\
& \left. + (\phi^J \parallel \{ P_{12}, r_4^2 \gamma_2(\alpha_4) \} \parallel \phi^{J'}) \right]
\end{aligned}$$

where $\{A, B\} \equiv A^\dagger B + B^\dagger A$

and use has been made of

$$\begin{aligned}
(\phi^J \parallel P_{1i}^\dagger r_i^2 \gamma_2(r_i) P_{ij} \parallel \phi^J) & \simeq (\phi^J \parallel P_{1i}^\dagger r_j^2 \gamma_2(r_j) \parallel \phi^J) \\
& \simeq (\phi^J \parallel P_{12}^\dagger r_j^2 \gamma_2(r_j) \parallel \phi^J)
\end{aligned}$$

where $i \neq j$ and $i \neq 2, j \neq 2$.

From the previous section, we know

$$\frac{2}{\sqrt{(2J'+1)}} \sum_{i=2}^4 (\Psi_J \| r_i^2 \gamma_2(\alpha_i) \| \Psi_{J'}) = Q_{12c}$$

$$\frac{2}{\sqrt{(2J'+1)}} (\Psi_J \| r_1^2 \gamma_2(\alpha_1) \| \Psi_{J'}) = Q_\alpha$$

and

$$B(E1, \alpha) = \left[\frac{1}{\sqrt{(2J'+1)}} (\Psi_J \| \frac{1}{e} \sum_{j=1}^4 e_j r_j^2 \gamma_2(\alpha_j) \| \Psi_{J'}) \right]^2$$

we can get

$$\begin{aligned} B(E1, \alpha) = & \left\{ N^J N^{J'} \left[4Q_\alpha + 4Q_{12c} + \frac{6}{\sqrt{(2J'+1)}} (\Phi^J \| 2r_1^2 \gamma_2(\alpha_1) P_{12} \| \Phi^{J'}) \right. \right. \\ & + 6Q_{12c} \langle \Phi^{J'} | P_{12} | \Phi^{J'} \rangle + \frac{6}{\sqrt{(2J'+1)}} (\Phi^J \| P_{12}^+ 2r_1^2 \gamma_2(\alpha_1) \| \Phi^{J'}) \\ & \left. \left. + 6 \langle \Phi^J | P_{12} | \Phi^J \rangle Q_{12c} \right] \right\}^2 \end{aligned} \quad (6)$$

where use has been made of

$$P_{12} |\Phi^J\rangle \simeq P_{13} |\Phi^J\rangle \simeq P_{14} |\Phi^J\rangle$$

(i.e., assuming the 1^2_C core is totally symmetric)

and

$$\frac{2}{\sqrt{(\omega^J+1)}} \sum_{i=2}^4 (\phi^J \| \gamma_i^2 \gamma_2(\omega_i) \| P_{12} \phi^{J'}) \simeq Q_{12C} \langle \phi^{J'} | P_{12} | \phi^{J'} \rangle$$

Here $\langle \psi^J | P_{12} | \psi^J \rangle$ is just EC^J defined in the previous section, so we can write

$$\begin{aligned} B(E\ell, \omega) = & \left\{ N^J N^{J'} \left[4Q_1 + 4Q_{12C} + 6 \frac{1}{\sqrt{(\omega^J+1)}} (\phi^J \| 2r_1^2 \gamma_2(\omega) P_{12} \| \phi^{J'}) \right. \right. \\ & + 6 Q_{12C} \times EC^{J'} + \frac{6}{\sqrt{(\omega^J+1)}} (\phi^J \| P_{12}^+ 2r_1^2 \gamma_2(\omega) \| \phi^{J'}) \\ & \left. \left. + 6 EC^J \times Q_{12C} \right] \right\}^2 \end{aligned}$$

where N^J is defined in the previous section.

Note that the matrix element reduces to the unsymmetrized matrix element in the limits where $P_{12} |\phi^{J'}\rangle$ vanishes, i.e.,

$$B(E\ell, \omega) = [Q_1 + Q_{12C}]^2 \quad (6a)$$

and if we approximate

$$(\phi^J \| \theta P_{12} \| \phi^{J'}) \simeq (\phi^J \| \theta \| \phi^{J'}) EC^{J'}$$

and

$$(\phi^J \| P_{12} \theta \| \phi^{J'}) \simeq EC^{J'} (\phi^J \| \theta \| \phi^{J'}), \text{ if } EC^{J'} > EC^J$$

we get

$$B(E\ell, \omega) \simeq \left\{ N^J N^{J'} [4 + 12 EC^{J'}] \times [Q_1 + Q_{12C}] \right\}^2$$

(6b)

Mean Square Radius with Full Exchange

Using the same notations we used in the previous section, we can find

$$\begin{aligned}
 \langle \Psi_J | r_i^2 | \Psi_{J'} \rangle &= N^J N^{J'} \left[\langle \phi^J | r_i^2 | \phi^{J'} \rangle + \sum_{i=2}^4 \langle \phi^J | r_i^2 | \phi^{J'} \rangle \right. \\
 &\quad + \langle \phi^J | r_i^2 (P_{i2} + P_{i3} + P_{i4}) | \phi^{J'} \rangle + \langle \phi^J | (P_{i2} + P_{i3} + P_{i4})^+ r_i^2 | \phi^{J'} \rangle \\
 &\quad \left. + \langle \phi^J | \{ P_{i2}, r_i^2 \} | \phi^{J'} \rangle + \langle \phi^J | \{ P_{i3}, r_i^2 \} | \phi^{J'} \rangle + \langle \phi^J | \{ P_{i4}, r_i^2 \} | \phi^{J'} \rangle \right] \\
 &= N^J N^{J'} \left[\langle \phi^J | r_i^2 | \phi^{J'} \rangle + \sum_{i=2}^4 \langle \phi^J | r_i^2 | \phi^{J'} \rangle + 3 \langle \phi^J | r_i^2 P_{i2} | \phi^{J'} \rangle \right. \\
 &\quad + 3 \langle \phi^J | P_{i2}^+ r_i^2 | \phi^{J'} \rangle + 3 \langle \phi^J | r_i^2 | \phi^{J'} \rangle \langle \phi^{J'} | P_{i2} | \phi^{J'} \rangle \\
 &\quad \left. + 3 \langle \phi^J | P_{i2} | \phi^J \rangle \langle \phi^J | r_i^2 | \phi^{J'} \rangle \right] \quad (7)
 \end{aligned}$$

where use has been made of

$$\langle \phi^J | r_i^2 | \phi^J \rangle = \langle \phi^J | r_2^2 | \phi^J \rangle = \langle \phi^J | r_4^2 | \phi^J \rangle$$

and

$$\langle \phi^J | r_i^2 P_{i2} | \phi^{J'} \rangle \simeq \langle \phi^J | r_i^2 | \phi^{J'} \rangle \langle \phi^{J'} | P_{i2} | \phi^{J'} \rangle$$

Since

$$\begin{aligned}
 |\phi^J\rangle &= \sum_{L_1} \frac{R_{L_1}(r_1)}{r_1} |Y_L \otimes \Phi_{L_1}\rangle \\
 &= \sum_{\substack{L_1 \\ L_2}} \frac{R_{L_1}(r_1)}{r_1} \frac{u_{L_2}(r_2)}{r_2} |Y_L(\alpha) \otimes (Y_{L_1}(\alpha_2) \otimes Y_{L_2}(\beta_r))_{L_1}\rangle_J
 \end{aligned}$$

we can get

$$\begin{aligned}
 \langle \phi^J | r_1^2 P_{12} | \phi^{J'} \rangle &= \sum_{\substack{L_1 L_1' \\ J_1 J_1'}} \left[\int R_{L_1}^*(r_1) u_{L_1'}(r_1) r_1^2 dr_1 \right] \\
 &\times \left[\int u_{L_1'}^*(r_2) R_{L_1'}(r_2) dr_2 \right] U(L_1', J_1'; L_1) \delta_{L_1 L_1'}
 \end{aligned}$$

Note that Eqn. (7) reduces to the unsymmetrized matrix element in the limits where $P_{12} |\phi^{J'}\rangle$ vanishes, i.e.,

$$\langle \Psi_J | r_1^2 | \Psi_{J'} \rangle \approx \frac{1}{4} \left[\langle \phi^J | r_1^2 | \phi^{J'} \rangle + \sum_{i=2}^4 \langle \phi^J | r_i^2 | \phi^{J'} \rangle \right] \quad (7a)$$

and if we approximate

$$\langle \phi^J | r_1^2 P_{12} | \phi^{J'} \rangle = \langle \phi^J | r_1^2 | \phi^{J'} \rangle EC^{J'}$$

and

$$\langle \phi^J | P_{12} r_1^2 | \phi^{J'} \rangle = EC^J \langle \phi^J | r_1^2 | \phi^{J'} \rangle$$

we can get

$$\begin{aligned}
\langle \Psi_J | r_i^2 | \Psi_{J'} \rangle &= N^J N^{J'} \left[\langle \phi^J | r_i^2 | \phi^{J'} \rangle + \sum_{i=2}^4 \langle \phi^J | r_i^2 | \phi^{J'} \rangle \right. \\
&\quad + 3 \left(\langle \phi^J | r_1^2 | \phi^{J'} \rangle + \langle \phi^J | r_2^2 | \phi^{J'} \rangle \right) E_C^{J'} \\
&\quad \left. + 3 \left(\langle \phi^J | r_1^2 | \phi^{J'} \rangle + \langle \phi^J | r_2^2 | \phi^{J'} \rangle \right) E_C^J \right] \quad (7b)
\end{aligned}$$

Here the r_1 should represent the distance between the center of mass of the ^{16}O and the i^{th} α particle. However, in our calculation, we calculate the distance between the center of mass of the ^{12}C and the i^{th} α particle. In order to transform the $\langle r_i \rangle$ from the center of mass system to our system, we need the following transformation,

$$\begin{aligned}
\langle r_i \rangle_{\text{CM}} &= \frac{3}{4} \langle r_i \rangle \\
\langle r_i \rangle_{\text{CM}} &= \sqrt{\left(\frac{\langle r_i \rangle^2}{4} + \langle r_2 \rangle^2} \quad , \quad i \neq 1
\end{aligned}$$

To include the finite size of the α particle, we use the following equations,

$$\langle a | R_i^2 | b \rangle = \langle a | r_i^2 | b \rangle + \langle a | R_\alpha^2 | b \rangle \delta_{ab}$$

where R_α is the radius of the α particle (1.7 fm).

In our calculation, we put the value of the radius of the ^{12}C core as our value of $\langle \psi^J | r_1^2 | \psi^J \rangle$, ($i \neq 1$)

Width of the Resonance

If the interior wave function is calculated and joined smoothly into the exterior solution at $r=a$, the phase shifts can be expressed in terms of the logarithmic derivatives at the boundary $r=a$:

$$\beta_l = \left(\frac{a}{R_l} \frac{dR_l}{dr} \right)_{r=a}$$

where R_l is the interior wave function with angular momentum l .

If the exterior solution is the Coulomb wave, then we can introduce the real parameter S_l by

$$S_l = \text{Im} \left[ka \frac{F_l' + i G_l'}{F_l + i G_l} \right]$$

where F_l is the regular Coulomb wave

G_l is the irregular Coulomb wave

k is the wave number.

If the rapid change of the phase shift β_l in a small energy range can be represented by a linear approximation:

$$\beta_l(E) = c + bE$$

then the width of the resonance can be written as³⁸

$$\Gamma = -2 \frac{S_l}{b}$$

CHAPTER III

Numerical Details

The calculation of the potential matrix elements is straight forward. We first project the effective potential V_{12C}^m (Eqn. 3) onto the basis Y_1^m and find each component V_1^m (Eqn. 4). In integrating Equation (4), we used Simpson's Rule with 20 points in ϕ direction (from 0 to π) and with 40 points in θ direction (from 0 to $\frac{\pi}{2}$). The size of basis that we require to give a good representation will be discussed in the next chapter.

After we found the V_1^m , we can use Equation (5a) to calculate the right hand side of Equation (5). Let us rewrite it to be

$$R_{L_n I_n}^{J''}(r) = \sum_{L'_n I'_n} Q_{L'_n I'_n}^{L_n I_n}(r) R_{L'_n I'_n}^J(r)$$

where $R_{L_n I_n}^{J''}(r)$ is the second derivative of $R_{L_n I_n}^J(r)$ with respect to r , and we have combined the $\frac{L_n(L_n+1)}{r^2}$ and E_n terms into $Q_{L'_n I'_n}^{L_n I_n}(r)$

Remember the matrix elements are functions of r . So if we have five channels for the wave function and we want to calculate the wave function between 0 and 7 fm in the step of 0.05 fm, we will have $5 \times 5 \times \frac{7}{0.05} = 3,500$ matrix elements to calculate. For our Sigma 7 computer, it takes about 4 minutes to calculate all these if $V_{\alpha^{-12}C}$ is independent of ϕ , otherwise it takes about 25 minutes to calculate. Once all matrix elements are calculated, we put them in file for later use in the coupled channels equations (CCE). To solve the CCE, we first have the boundary conditions for each channel wave function at $r=0$ and $r=r_{\max}$ (where r_{\max} is the outside limit of the wave function, in our calculation $r_{\max} = 7$ fm). Let us symbolize these wave function as

$$\underline{\underline{u}}^{\text{inner}}(r)$$

where the superscription "inner" denotes that they solve the Schroedinger equation in the inner region with $0 < r < r_{\text{in}}$ (we use the Noumerov method³⁹ to solve the differential equation), and the underlines denote that the wave function at any given radial mesh point r_M is a matrix in the space of (initial values = n) \times (channels = m). In a similar way we can define $\underline{\underline{u}}^{\text{outer}}(r)$ for $r_{\text{in}} < r < r_{\text{max}}$ integrating inward from r_{max} . We wish to match the wave function at r_{match} in each channel, so we perform a linear transformation on $\underline{\underline{u}}^{\text{outer}}(r)$, i.e. $\underline{\underline{w}}^{\text{outer}}(r) = \underline{\underline{A}} \times \underline{\underline{u}}^{\text{outer}}(r)$ with $\underline{\underline{A}} = \underline{\underline{u}}^{\text{inner}}(r_{\text{match}}) \times (\underline{\underline{u}}^{\text{outer}}(r_{\text{match}}))^{-1}$. The wave function $\underline{\underline{u}}^{\text{inner}}$

matches $\underline{w}^{\text{outer}}$, but do not join smoothly, i.e. $(\underline{u}^{\text{inner}}(r_{\text{match}}))' \neq (\underline{w}^{\text{outer}}(r_{\text{match}}))'$. If $m = n+1$, we can define an $(m-1)$ dimensional vector \underline{B} from the following equation:

$$(\underline{u}^{\text{inner}}(r_{\text{match}}) - \underline{w}^{\text{outer}}(r_{\text{match}})) \times \underline{B} = 0$$

Once \underline{B} is found, the first $(m-1)$ channel wave functions

$$\underline{v}^{\text{inner}} = \underline{B} \times \underline{u}^{\text{inner}}$$

$$\text{and } \underline{v}^{\text{outer}} = \underline{B} \times \underline{w}^{\text{outer}}$$

will join smoothly at the match point. The last channel wave function usually will not join smoothly unless E_n in Eqn. (5) is indeed the eigenvalue. So in order to determine the eigenvalue E_n and solve the CCE, we have to vary the E_n until this channel wave function joins smoothly.

There are a few tricks we needed in using the program in order that the E_n converge quickly to the eigenvalue. First, we match the wave which contributes most to the total wave function. Secondly, we choose the match point close to the peak of the wave. The program usually searches 4 times until it converges to within 10^{-4} MeV of the eigenstate. In Table (4), we show the time needed for each search versus different number of channels.

CHAPTER IV

Energy Spectra, Wave Functions and Physical Properties

In Chapter II, we showed that if we know the structure of ^{12}C and the α - α potential, we can calculate the α - ^{12}C effective potential. The simplest α -model of ^{12}C is a static triangle^{6,7,8} formed by the 3α particles. Let us choose the Z axis to be the symmetric axis of the triangle,⁴⁰ then the $\rho(\Omega)$ in Eqn. (3) becomes

$$\rho(\Omega) = C \sum_{i=1}^3 \delta(r-r_0) \delta(\theta - \frac{\pi}{2}) \delta(\phi - \frac{2\pi}{3}(i-1))$$

where C satisfies
$$\int \rho(\Omega) d\Omega = 3$$

and r_0 is the radius of the ^{12}C in α -particle model (we choose $r_0 = 1.85$ fm).

Because of the structure of the ^{12}C , the sum over l and m in Eqn. (4) is limited to those which satisfy the symmetry properties of a triangle (i.e., $Y_{L=\text{even}}^0$ or Y_1^m , where $l+m = \text{even}$; $m=3xn$ and n is interger number). In determining how many terms we needed in the summation to give a good representation when we used the Ali & Bodmer potential, we

found that with $Y_{L,0}$ ($L = 0, 2, 4, 6, 8, 10, 12$), $Y_{3,\pm 3}$, $Y_{5,\pm 3}$, and $Y_{6,\pm 6}$ terms, Eqn. (4) gives a good representation of the effective potential (in a sense that the projected potential differs from the actual potential by less than 10% at the valley of the potential and less than 1% at other point of the potential). Later when we used the stronger potential--Neudatchin potential³³ and Vary & Dover potential,³⁴ we only used $U_{L,0}$ ($L = 0, 2, 4, 6, 8, 10, 12$) terms in Eqn. (4).

For the α - α potential, we first used the Ali and Bodmer potential.²⁹ This potential has a short-range repulsion and L-dependence which come from the exclusion effect. Because this potential is L-dependent, there will be some difficulties in carrying out the calculation. First, in the expansion of the potential (Eqn. (4)), we expand it in the basis of Y_{1m} , where l is the angular momentum of the relative motion between the α particle and the center of mass of the ^{12}C , not the angular momentum of the relative motion between the individual α - α pair. Secondly, we don't know the magnitude of each component of the potential. For the first problem, we assume the ^{12}C core is rigid enough such that we can approximate the $Y_{1,m}$ in Eqn. (4) to be the relative motion of the α - α pair. For the second problem, we first calculate the wave function of the system by assuming the relative motion is in the S state only. After we find the wave function, we can find the mixing of the potential. Using this information we can

find a new potential and recalculate the wave function. In principle we can do this repeatedly until we get a self-consistent potential.

In Figure 2, we show the spectra for Ali-Bodmer potential (only the states that have positive exchange matrix elements (see Chapter II) are shown) and the experimental result. It can be seen that although the states are in the right order, the binding energy of the ground state is only about 71% of the experimental value. The excitation 0^+ state is unbound by 1.7 MeV while in experiment it is bound by 1.48 MeV. In Mendez and Seligram's calculations,²⁷ they also encountered the underbound problem and they concluded that the α - α potential determined by the phase shift methods is not strong enough to give the right binding of the nucleus. To investigate the potential, we first increased the depth of the potential without changing other parameters and we show the result in Figure 3. It can be seen the ground state now becomes overbound if we want the first excited 0^+ state to be bound at the right amount of energy. We also tried Benn & Scharf's potential⁴¹ and Chien's potential.⁴² But these two potentials are similar to the Ali and Bodmer's, they give results similar to Ali and Bodmer's.

Since we believe the underbinding of the nucleus is due to the fact that the potential is not strong enough, so in the next step, we use the deep potentials suggested by Neudatchin³³ and by Vary and Dover.³⁴ This type of potential

is somewhat simpler for it is L-independent. But because it does not include the exclusion effect explicitly, it usually induces a lot of spurious states and we have to be very careful in choosing the true states. In the resonating-group calculation on two alpha particles system,⁴³ the wave function for the lowest state that describes the relative motion of the two alpha particles has two nodes. To show that this argument is consistent with the shell model,^{43,14} first let us describe the spatial behavior of the two α clusters by

$$\phi_1 = \exp \left[-\frac{1}{2} a \sum_{i=1}^4 (r_i - R_1)^2 \right]$$

$$\phi_2 = \exp \left[-\frac{1}{2} a \sum_{i=5}^8 (r_i - R_2)^2 \right]$$

where R_1 and R_2 are the position vectors of the center of mass of the two α clusters respectively and a is the width of the oscillator well. Secondly, let us describe the relative motion of the two alpha clusters by the function

$$g(r) = C Y \left[1 - \frac{8}{3} ar^2 + \frac{16}{15} a^2 r^4 \right] e^{-ar^2}$$

where C is the normalization factor.

Using these notations, we found the usual shell model wave function describing the lowest configuration $(1s)^4(lp)^4$ can be written as

$$\Psi_{l=0} = A \left[\phi_1 \phi_2 \frac{g(r)}{r} \xi(\sigma, \tau) \right]$$

where A is the antisymmetrization operator and $\xi(\sigma, \tau)$ denotes the appropriate charge-spin function.

It is clear the function $g(r)$ has two nodes and we have shown the argument is consistent with the shell model.

Since we know in α -particle model the α configuration of $^{16}_0$ in ground state is a regular tetrahedron,⁵ so in the $\alpha+^{12}_6\text{C}$ system if we put the $^{12}_6\text{C}$ on the x-y plane, the extra α particle should be peaked along the Z axis. If we consider the $^{12}_6\text{C}$ as a static triangle formed by the 3α particles, the wave function describing the relative motion of the $\alpha+^{12}_6\text{C}$ should have 4 nodes along the Z axis. This is how we identify the ground state of $^{16}_0$.

To identify the 0_2^+ state, we follow the argument given by Terasawa, et al.⁹ In the $^{20}\text{Ne}(d, ^6\text{Li}) ^{16}_0$ reaction, both the 0_1^+ and 0_2^+ states are strongly excited. This can be interpreted as the pick up of four particles from the 2s-1d shell for the 0_1^+ state, and the pick up of four particles from the lp shell for the 0_2^+ state. Since our model describes $^{16}_0$ as an α particle plus a $^{12}_6\text{C}$, the α -particle in the 0_2^+ state will consist of four nucleons in the 2s-1d shell. This four-particle excitation gives four for the number of nodes of the

α -particle wave function in this state. Also we know that the α -configuration of ^{16}O in the 0_2^+ state is a plane diamond.⁵ If the ^{12}C is lying on the x-y plane, the extra α particle should be peaked on the x-y plane and the number of nodes of the wave function describing the relative motion of the $\alpha + ^{12}\text{C}$ should be four along the x-y plane. This is how we identify the 0_2^+ state of ^{16}O .

To project our wave function into the coordinate space, we approximate the internal wave function of the ^{12}C as the rotor model wave function. Because we put the ^{12}C core on the x-y plane, the wave function in coordinate space can be written as

$$\Psi_{J=0}(r, \theta) = \sum_l \frac{R_{ll}(r)}{r} Y_{l,0}(\omega\theta)$$

where r, θ refer to the α coordinates in the space fixed system.

and the probability of the α particle located along θ degree is

$$P_0(\theta) = \int |P(r, \theta)|^2 r^2 dr$$

where

$$P(r, \theta) = |\Psi_{J=0}(r, \theta)|^2$$

No attempt has been made to identify the 2^+ and 4^+ states, because we no longer have enough basis to describe the internal

wave function of the ^{12}C . But by looking at the $B(E2)$ transition rates and the α decay widths, we can identify the physical 2^+ and 4^+ states.

In Figure 3, we show the spectrum we got for the Neudatchin potential³³ and the folded potential by Vary and Dover.³⁴ We can see the bound states in both spectra are overbound. For the folded potential, the depth of the potential was originally adjusted to fit the $\alpha + ^{16}\text{O}$ elastic scattering data, therefore it is very likely that the potential is too deep for the α - α potential. We adjust the potential's depth to fit the binding energy of the ground state and get the spectrum shown in Figure 4. The over all fit of the spectrum is good. We plot the probability of the α particle versus the angle between the α particle and the ^{12}C core in Figure 10 and Figure 11 (in these figures, solid lines represent the folded potential by Vary and Dover, dashed lines represent the Ali and Bodmer potential and dotted-dashed lines represent the Heudatchin potential). Figure 10 shows that the α configuration of the ^{16}O in ground state is a tetrahedron. Figure 11 shows that the α configuration of the ^{16}O in the first excited 0^+ state tends to be a plane diamond for the deep potential, but tends to be a mixture between the plane diamond and the tetrahedron for the Ali and Bodmer potential. This is because the Ali and Bodmer potential is too weak to produce a bound 0_2^+ state. This is another evidence that the Ali and Bodmer potential is not suitable in the structure calculation.

The ground state wave function and the 0_2^+ state wave function for Ali and Bodmer potential are shown in Fig. 12 and Fig. 13. The ground state wave function and the 0_2^+ state wave function for the Folded potential are shown in Fig. 14 and Fig. 15. In these figures, only the two most important components of the wave function are shown.

In Table 5 we show the probabilities of the wave function for different potentials and the probabilities calculated by Noble and Coelho.³¹ In Table 6 we show the exchange matrix elements for the states of different potentials. Here we only show those with positive sign, those with negative sign that violate the symmetric property of the nucleus are not shown in the table.

The mean square radii (Eqn. 7) (Eqn. 7a) (Eqn. 7b) and the B(E2) transition rates (Eqn. 6) (Eqn. 6a) (Eqn. 6b) are shown in Table 9 and Table 10a. All mean square radii agree very well with experimental results. The mean square radii for the repulsive core potential are larger than those for the deep potentials. That is because the different shapes of the two potentials. The B(E2) transitions for the repulsive core potentials are larger than those for the deep potentials. The repulsive core potential predicts an excessively large transition strength to the 0_2^+ state, while the deep potentials predict too small a transition rate as expected. We compare the B(E2) predicted by the deep potential and the B(E2) from Brown's shell model calculation in Table

10b. The shell model predicts an excessively large $B(E2)$, while the α model with a deep α - α potential predicts too small a $B(E2)$

We use the formalism mentioned in Chapter II to calculate the width of resonance. To check the result, we also calculate the width by using the R-matrix formalism by Arima and Yoshida.⁴⁶ It turns out that both results agree within 10%. Since the width is very sensitive to the energy of the state, in order to compare the width with the experimental value,⁴⁷ we have to adjust the α - α potential by the method we mentioned before to get the energy of the state close to the experimental value. We list our results together with the experimental results in Table 11. The width we got for the 4^+ state is only about 50% of the experimental value,⁴⁷ while the width for the 2^+ state is almost three times bigger than the experimental result. But considering the crude calculation we had for the decay width, it is quite satisfactory that the results are in the right order of magnitude.

CHAPTER V

Summary and Conclusion

We start by assuming the ^{16}O is made up of a ^{12}C core plus an α particle. We use different realistic α - α potentials to determine the effective α - ^{12}C potential. In determining the effective α - ^{12}C potential, we only consider the pair wise α - α potential and neglect all the higher order interactions (e.g., three-body interaction). For the structure of the ^{12}C , we assume the 3α particles are in a triangular configuration. The size of the triangle is determined by electron scattering. No intrinsic excited states of ^{12}C are being considered. Knowing the structure of the ^{12}C and the α - α potential, we can find the effective α - ^{12}C potential.

We put the wave function of the system in a weak coupling model form, use the effective α - ^{12}C potential, and find a set of coupled-channel equations from the Schrodinger equation. By solving the coupled-channel equation, we find that the bound states of the nuclei are underbound for the weak α - α potentials and become overbound when we use the deep α - α potentials. By adjusting the depth of the folded potential of Vary and Dover, we can find the correct binding of the nuclei and still get a spectrum that fits the experimental result reasonably well. Therefore, the deep potential

is qualitatively more realistic than the weak potential for structure calculations in α -particle model.

Unfortunately, one problem of the deep potential is that it induces a lot of spurious states. We find the physical states by choosing the states that have the right number of nodes in their wave functions and satisfy the Bose-Einstein statistics. In considering the problem of wave function symmetry, we find the exchange matrix elements (see Chapter II) are smaller than +1; the reason for this is presumably because of the inadequacy of basis: no intrinsic excited states of ^{12}C are being considered. To remedy this defect, we derive some formulas in Chapter II to calculate different physical properties (except the α -width). From our results we show that the α - α scattering data do not sufficiently determine the interaction to make predictions on the structure of more complicated nuclei. The interactions with repulsive cores give a very smooth structure to the states and tend to underbind the ground state. Also the transition rates to the 0_2^+ state are too large. The deep attractive interactions suffer from opposite defects. The states are now overbound, and differ from each other to such an extent that the transition rates are an order of magnitude too small. Of the two types of interaction, we prefer the deep potential, because the structure of the states matches the more fundamental cluster model.

REFERENCES

REFERENCES

1. D. R. Inglis, Rev. Mod. Phys. 25(1953)390.
2. J. C. Bergstrom, et al., Phys. Rev. Lett. 24(1970)152.
3. G. J. Stephenson, M. K. Banerjee, Phys. Lett. 24B(1967)209.
4. G. E. Brown, A. M. Green, Nucl. Phys. 75(1966)401;
G. E. Brown, Proc. to the Int. School of Phys. "Enrico Fermi" Course 36.513.
5. G. F. Bertsch, W. Bertozzi, Nucl. Phys. A165(1971)199.
6. D. M. Brink, et al., Phys. Lett. 33(1970)143.
7. P. S. Hauge, Thesis (Iowa State University).
8. N. Takigawa, and A. Arima, Nucl. Phys. A168(1971)593.
9. T. Terawasa, M. Tanifuji, and O. Mikoshiba, Nucl. Phys. A203(1973)225.
10. G. Gamow, Proc. Roy. Soc. A126(1930)632.
11. G. Breit and I. Rabi, Phys. Rev. 46(1934)230; L. R. Hafstad and E. Teller, Phys. Rev. 54(1938)681.
12. N. Bohr, Nature 137(1936)344.
13. H. Margenau, Phys. Rev. 59(1941)37.
14. D. Brink, Proc. of the Int. Sch. of Phys., Course 36, 247.
15. S. J. Biel, Proc. Phys. Soc. A70(1957)866.
16. C. Abulaffio and J. M. Irvine, Phys. Lett. 34B(1971)492.

17. W. Wefelmeier, *Naturwiss*, 25(1937)525.
18. J. A. Wheeler, *Phys. Rev.* 52(1937)1083.
19. D. Dennison, *Phys. Rev.* 57(1940)454; 96(1954)378.
20. S. L. Kameny, *Phys. Rev.* 103(1956)358.
21. J. K. Perring, T.H.R. Skyrme, *Proc. Phys. Soc.* A69
(1956)600.
22. E. Teller, and J. A. Wheeler, *Phys. Rev.* 53(1938)778;
J. A. Wheeler, *Phys. Rev.* 52(1937)1083.
23. S. Edwards, *Proc. Cam. Phil. Soc.* 48(1952)652.
24. K. Wildermuth and T. Kanellopoulos, *Nucl. Phys.* 9(1958)
449.
25. Z. Matthies, V. G. Neudatchin, Yu. F. Smituov,
Zurn. Fksp. Ter. Fiz. 45(1963); *Nucl. Phys.* 49(1963)97.
26. A. Y. Abul-Magd, *Nucl. Phys.* A129(1969)610.
27. R. M. Mendez, and T. H. Seligman, *Phys. Lett.* 36B(1973)
307; *Nucl. Phys.* A221(1973)381.
28. M. Moshisky, "The Harmonic Oscillator in Modern Physics
from Atoms to Quarks", Gordon and Breach, N.Y. (1969);
V. C. Aquilera-Navarro, M. Moshisky, and P. Kramer,
Ann. Phys. (N.Y.) 51(1969)512; *Ann. Phys. (N.Y.)* 54(1969)
379.
29. S. Ali, A. R. Bodmer, *Nucl. Phys.* 80(1966)99.
30. J. V. Noble, *Phys. Rev.* C1(1970)1900.
31. J. V. Noble, and H. J. Coelho, *Phys. Rev.* C3(1971)1840.

32. B. Tatischeff and I. Brissand, Nucl. Phys. A155(1970) 89.
33. V. G. Neudatchin, Phys. Lett. 34B(1971)581.
34. J. P. Vary and C. B. Dover, Phys. Rev. Lett. 31(1973)1510.
35. A. K. Kerman, H. McManus and R. M. Thaler, Ann. Phys. 8(1959)551.
36. M. Rose, "Elementary Theory of Angular Momentum".
37. A. Shalit and I. Talmi, "Nuclear Shell Theory".
38. E. Merzbacher, "Quantum Mechanics".
39. B. V. Noumerov, Monthly Notices Roy. Astron. Soc. 84 (1924)592; Publ. Observ. Astrophys. Central Russie 2 (1923)188.
40. S. Das Gupta and N. deTakacsy, Phys. Rev. Lett. 22(1969) 1194.
41. J. Benn and G. Scharf, Helv. Phys. Acta. 40(1967)271.
42. J. Chien, Thesis (University of Minnesota) 1973.
43. D. R. Thompson, I. Reichstein, W. McClure, and Y. C. Tank, Phys. Rev. 185(1969)1351.
44. J. V. Noble, Phys. Lett. 31B(1970)253.
45. J. Borysowicz, Phys. Lett. 35B(1971)113.
46. A. Arima and S. Yoshida, Nucl. Phys. A219(1974)475.
47. C. M. Jones, et al., Nucl. Phys. 37(1962)1.
48. G. W. Greenlees, G. J. Pyle, and Y. C. Tang, Phys. Rev. 171(1968)1115.
49. A. P. Zuker, B. Buck, J. B. McGrory, Phys. Rev. Lett. 21(1968)39.

50. F. Ajzenberg-Selove, Nucl. Phys. A166(1971)1.

APPENDICES

APPENDIX A

$$\begin{aligned}
 & \langle (LI)_{JM} | \sum_{\rho m k} Y_{\rho k}(\theta, \phi) D_{km}^{\rho}(\theta_i, \phi_i) | (L'I')_{JM} \rangle \\
 &= (-1)^{L+I+L'+I'} (\alpha J+1) \sum_{\rho m k} \sum_{\substack{m_1, m_2 \\ m'_1, m'_2}} (-1)^{m_1} \begin{pmatrix} L & I & J \\ m_1 & m_2 & -M \end{pmatrix} \begin{pmatrix} L' & I' & J \\ m'_1 & m'_2 & -M \end{pmatrix} \\
 & \quad \times \begin{pmatrix} L & l & L' \\ -m_1 & m & m'_1 \end{pmatrix} \begin{pmatrix} L & l & L' \\ 0 & 0 & 0 \end{pmatrix} \sqrt{\frac{(\alpha L+1)(\alpha l+1)(\alpha L'+1)}{4\pi}} \langle I M_2 | D_{km}^{\rho} | I' m'_2 \rangle
 \end{aligned}$$

Represent the $|IM\rangle$ wave function by a rotational matrix $\sum_x D_{Mx}^I$, the $\langle I M_2 | D_{km}^{\rho} | I' m'_2 \rangle$ can be solved, i.e.,

$$\langle I M_2 | D_{km}^{\rho} | I' m'_2 \rangle = \sum_{x x'} 8\pi^2 (-1)^{M_2+x} \begin{pmatrix} I' & l & I \\ m'_2 & k & -m_2 \end{pmatrix} \begin{pmatrix} I' & l & I \\ x' & m & -x \end{pmatrix}$$

and

$$\begin{aligned}
 & \langle (LI)_{JM} | \sum_{\rho m k} Y_{\rho k}(\theta, \phi) D_{km}^{\rho}(\theta_i, \phi_i) | (L'I')_{JM} \rangle \\
 &= (-1)^{L'+I'+L+I} (\alpha J+1) \sum_{x x'} \sum_{\rho m k} \sum_{\substack{m_1, m_2 \\ m'_1, m'_2}} 8\pi^2 \sqrt{\frac{(\alpha L+1)(\alpha l+1)(\alpha L'+1)}{4\pi}} \\
 & \quad \times (-1)^{m_1+m_2+x} \begin{pmatrix} L & I & J \\ m_1 & m_2 & -M \end{pmatrix} \begin{pmatrix} L' & I' & J \\ m'_1 & m'_2 & -M \end{pmatrix} \begin{pmatrix} L & l & L' \\ -m_1 & m & m'_1 \end{pmatrix} \begin{pmatrix} L & l & L' \\ 0 & 0 & 0 \end{pmatrix} \\
 & \quad \times \begin{pmatrix} I' & l & I \\ m'_2 & k & -m_2 \end{pmatrix} \begin{pmatrix} I' & l & I \\ x' & m & -x \end{pmatrix} \delta_{x'+m, x}
 \end{aligned}$$

Normalize the wave $|IM\rangle$ (i.e., $D_{mX}^I \rightarrow$
and make use of the following relation

$$\frac{D_{mX}^I}{\sqrt{\frac{8\pi^2}{(2I+1)}}}$$

$$\left\{ \begin{matrix} j_1 & j_2 & j_3 \\ l_1 & l_2 & l_3 \end{matrix} \right\} = \sum_{\substack{m_1, m_2, m_3 \\ m'_1, m'_2, m'_3}} (-1)^{j_1 + j_2 + j_3 + l_1 + l_2 + l_3 + m_1 + m_2 + m_3 + m'_1 + m'_2 + m'_3}$$

$$\times \begin{pmatrix} j_1 & j_2 & j_3 \\ m_1 & m_2 & m_3 \end{pmatrix} \begin{pmatrix} j_1 & j_2 & l_3 \\ -m'_1 & m'_2 & -m'_3 \end{pmatrix} \begin{pmatrix} l_1 & j_2 & l_3 \\ -m'_1 & -m_2 & m'_3 \end{pmatrix} \begin{pmatrix} l_1 & l_2 & j_3 \\ m'_1 & -m'_2 & -m_3 \end{pmatrix}$$

we can get

$$\begin{aligned} & \langle (LI)_{JM} | \sum_{l m k} Y_{lm}(\theta\phi) D_{km}^l(\theta_i, \phi_i) | (L'I')_{JM} \rangle \\ &= \sum_{\substack{L I \\ l m \\ X'}} (-1)^{J+l+m+L+L'+I} \sqrt{\frac{(2L+1)(2L'+1)(2I+1)}{4\pi(2J+1)(2l+1)}} (L'00|l0) \\ & \quad \times (I'lX'm|IX) U(LI, L'I'; J l) \delta_{X'+m, X} \end{aligned}$$

APPENDIX B

$$|\Psi_{J'}\rangle = \sum_{\substack{L_1' I_1' \\ L_2' I_2'}} \frac{R_{L_1'}(r_1)}{r_1} \frac{u_{L_2'}(r_2)}{r_2} |\gamma_{L_1'}(\alpha_1) \otimes (\gamma_{I_1'}(\alpha_1) \otimes \gamma_{I_2'}(\beta_2))_{I_1'}\rangle_{J'}$$

$$\begin{aligned} P_{12}|\Psi_{J'}\rangle &= \sum_{\substack{L_1' I_1' \\ L_2' I_2'}} \frac{R_{L_1'}(r_2)}{r_2} \frac{u_{L_2'}(r_1)}{r_1} |\gamma_{L_1'}(\alpha_2) \otimes (\gamma_{I_1'}(\alpha_1) \otimes \gamma_{I_2'}(\beta_2))_{I_1'}\rangle_{J'} \\ &= \sum_{\substack{L_1' I_1' \\ L_2' I_2'}} \frac{R_{L_1'}(r_2)}{r_2} \frac{u_{L_2'}(r_1)}{r_1} U(L_1' I_1' J' I_2'; 2 I') \\ &\quad \times \left[\gamma_{L_1'}(\alpha_1) \otimes (\gamma_{L_1'}(\alpha_2) \otimes \gamma_{L_2'}(\beta_2))_{I_2'} \right]_{J'} \end{aligned}$$

$$\frac{1}{\sqrt{(2J'+1)}} \langle \Psi_{J'} \| r_1^\ell \gamma_\ell \| P_{12} \Psi_{J'} \rangle$$

$$= \frac{1}{\sqrt{(2J'+1)}} \sum_{\substack{L_1 I_1 \\ L_2 I_2}} \sum_{\substack{L_1' I_1' \\ L_2' I_2'}} \sum_{I'} \left[\int R_{L_1}(r_1) R_{L_2'}(r_1) r_1^\ell dr_1 \right]$$

$$\times \left[\int u_{L_2}(r_2) R_{L_1'}(r_2) dr_2 \right] U(L_1 I_1, J' I_2'; 2 I')$$

$$\times (\gamma_{L_1}(\alpha_1) \otimes (\gamma_{L_2}(\alpha_2) \otimes \gamma_{L_2})_{I_2} \| \gamma_\ell \| \gamma_{L_1}(\alpha_1) \otimes (\gamma_{L_2}(\alpha_2) \otimes \gamma_{L_2})_{I_2})$$

We know

$$\begin{aligned}
 & (Y_L(\alpha_1) \otimes \Phi_{I_1} \parallel Y_p(\alpha_1) \parallel Y_{I_1'}(\alpha_1) \otimes \Phi_{I_2}) \\
 = & (-1)^{L+I_1+J+I} \sqrt{(\partial J+1)(\partial J'+1)} \begin{Bmatrix} L & I_1' & I \\ J' & J & I \end{Bmatrix} \\
 & \times (Y_L(\alpha_1) \parallel Y_p(\alpha_1) \parallel Y_{I_1'}(\alpha_1)) \delta_{I_2 I_2'} \delta_{I_1 L'} ,
 \end{aligned}$$

$$\begin{aligned}
 & (Y_L(\alpha_1) \parallel Y_p(\alpha_1) \parallel Y_{I_1'}(\alpha_1)) \\
 = & (-1)^{-I_1'+I} \begin{pmatrix} I_1' & I & L \\ 0 & 0 & 0 \end{pmatrix} \left[\frac{(\partial I_1'+1)(\partial I+1)}{4\pi} \right]^{1/2} (\partial L+1)^{1/2}
 \end{aligned}$$

and

$$\begin{aligned}
 & U(L' I_1', J' I_2'; I I') \\
 = & (-1)^{L'+I_1'+J'+I_2'} \sqrt{(\partial L'+1)(\partial I'+1)} \begin{Bmatrix} L' & I_1' & I \\ I_2' & J' & I' \end{Bmatrix}
 \end{aligned}$$

we can get

$$\begin{aligned}
 & \frac{1}{\sqrt{(\partial J'+1)}} (\Psi_J \parallel r_1^I Y_L \parallel P_{I_2} \Psi_{J'}) = \sum_{\substack{L_1' \\ I_1' I_2'}} \sum_{\substack{L_2' \\ I_1' I_2'}} \left[\int R_{L_1'}(r_1) R_{I_1' I_2'}(r_1) r_1^I dr_1 \right] \\
 & \times \left[\int u_{I_2 I_2'}(r_2) R_{I_1' I_2'}(r_2) dr_2 \right] (-1)^{L'+J'+I_2'+L+I+J} \sqrt{\frac{(\partial I+1)(\partial I'+1)(\partial J+1)(\partial I'+1)}{4\pi}} \\
 & \times \sqrt{(\partial L+1)(\partial L'+1)} \begin{Bmatrix} L' & I_1' & I \\ I_2' & J' & I' \end{Bmatrix} \begin{Bmatrix} L & I_1' & I \\ J' & J & I \end{Bmatrix} \begin{pmatrix} I_1' & I & L \\ 0 & 0 & 0 \end{pmatrix} \delta_{I_2 I_2'} \delta_{I_1 L}
 \end{aligned}$$

TABLE 1.--Mixing ratios from TTM's calculation and present calculation.

J^{π}	Terasawa's Results				Present Results			
	0_2^+	2_1^+	2_2^+	2_3^+	0_2^+	2_1^+	2_2^+	2_3^+
s_{00}^+	85.3				84			
d_{00}^+		88.6	0.03	N.A.		84	0.02	0.4
s_{20}^+		1.7	29	N.A.		3	31	28
d_{20}^+	14	3.3	61.64	N.A.	16	5	61	5
g_{20}^+		6.3	9	N.A.		8	8	6.7

TABLE 2.--Volume integrals of various potentials (V_d being defined in (48)).

Type of Potential	V_d (MeV-fm ³)
A.B.* (L=0)	-20.25
A.B.* (L=2)	162.38
A.B.* (L=4)	487.06
A.B.* (L=SC) ⁺	79.3
Chien (L=SC) ⁺	117.13
Folded	318.2
Neudatchin	437.38
Folded (adjusted)	260.9

* AB = Ali and Bodmer

⁺ SC = Self-consistent

TABLE 3.--Ground state properties of ^{12}C and ^{16}O from Brink.⁶

Nucleus	B (MeV)	B_{hf} (MeV)	B_{exp} (MeV)	\bar{R} (fm)	\bar{R}_{hf} (fm)	\bar{R}_{exp} (fm)
^{12}C (triangle)	62		92.2	2.62		2.37
^{16}O (tetrahedron)	94.4	92.9	127.6	2.62	2.71	2.64

TABLE 4.--Computation times for the CCE program.

Number of channels	2	4	5
Time for Each Search	.04 sec	.17 sec	.27 sec

TABLE 5a.--Probabilities of various l in G.S. and 0_2^+ state for Ali and Bodmer potential, also the mixing ratios calculated by Noble and Coelho.³¹

J^π	N.C.*	A.B. Potential	
	G.S.	G.S.	0_2^+
$s_{\square}0^+$	N.A. ⁺	0.433	0.831
$d_{\square}2^+$	0.375	0.511	0.125
$g_{\square}4^+$	0.15	0.036	0.021
$f_{\square}3^-$	0.075	0.011	0.022
$h_{\square}5^-$	N.A. ⁺	0.008	0.0008

* N.C. = Noble and Coelho³¹

⁺N.A. = not available

TABLE 5b.--Probabilities of various l in G.S. and 0_2^+ state for Vary and Dover's folded potential.

J^π	Folded Potential	
	G.S.	0_2^+
$s_{\square}0^+$	0.0856	0.698
$d_{\square}2^+$	0.357	0.23
$g_{\square}4^+$	0.504	0.063
$i_{\square}6^+$	0.052	0.008
$k_{\square}8^+$	0.0016	0.0004

TABLE 6.--Exchange matrix elements.

Potential	State	G.S.	0_2^+	2_1^+
Ali and Bodmer		0.828	0.25	0.11
Neudatchen		0.126	0.12	0.283
Folded (Adjusted)		0.27	0.245	0.044

TABLE 7.--Ground state binding energies for different potentials.

	E(MeV)
Experiment	-7.16
Ali and Bodmer	-5.1
Neudatchen	-22.
Vary (adjusted)	-7.2

TABLE 8.--Excitation energies for different potentials.

	0_2^+	2_1^+
Experiment	-1.11 MeV	-0.142 MeV
Vary (adjusted)	-0.8 MeV	1.2 MeV

TABLE 9.--Mean square radii. *

	Exp. ⁵⁰	Alli and Bodmer		Folded (adjusted)		Neudatchen				
		Eqn. (7a)	Eqn. (7b)	Eqn. (7a)	Eqn. (7b)	Eqn. (7a)	Eqn. (7b)			
$\sqrt{\langle G.S. R^2 G.S. \rangle}$ (fm)	2.67	2.68	2.68	2.54	2.54	2.63	2.51	2.51	2.56	
$\langle G.S. R^2 0_2^+ \rangle$ (fm ²)	3.7	6.04	8.51	9.98	1.74	1.8	7.29	0.18	0.2	2.68
$\sqrt{\langle 0_2^+ R^2 0_2^+ \rangle}$ (fm)		3.05	3.05	3.18	2.85	2.85	3.02	2.78	2.78	2.92

* The finite size of the α particle are being considered, see Text.

TABLE 10a.--B(E2) transition rates.

B(E2)(e ² fm ⁴)	Ali and Bodmer		Folded (adjusted)		Neudatchen					
	Eqn. (6a)	Eqn. (6b)	Eqn. (6a)	Eqn. (6b)	Eqn. (6a)	Eqn. (6b)				
2 ₁ ⁺ →G.S.	7.28	10.1	1.77	0.94	0.003	.044	.05	.007		
2 ₁ ⁺ →0 ₂ ⁺	40±15	92.63	123.	55.16	44.6	68.	19.95	3.62	4.8	5.3

TABLE 10b.--Comparison of our B(E2) and Brown's B(E2)⁴.

B(E2) (e ² fm ⁴)	exp ⁵⁰	Folded* (Eqn. (6b))	A+B ⁺ (Eqn. (6b))	Brown ⁴
2 ₁ ⁺ →G.S.	8±1	0.94	0.53	5.3
2 ₁ ⁺ →0 ₂ ⁺	40±15	68.	39.6	103.

*Folded (adjusted)

⁺Ali and Bodmer (adjusted) (see figure.2)

TABLE 11.--α decay width.

State	Exp ⁵⁰	Vary (adjusted)
2 ⁺	1 kev	2.6 kev
4 ⁺	33 kev	16.3 kev

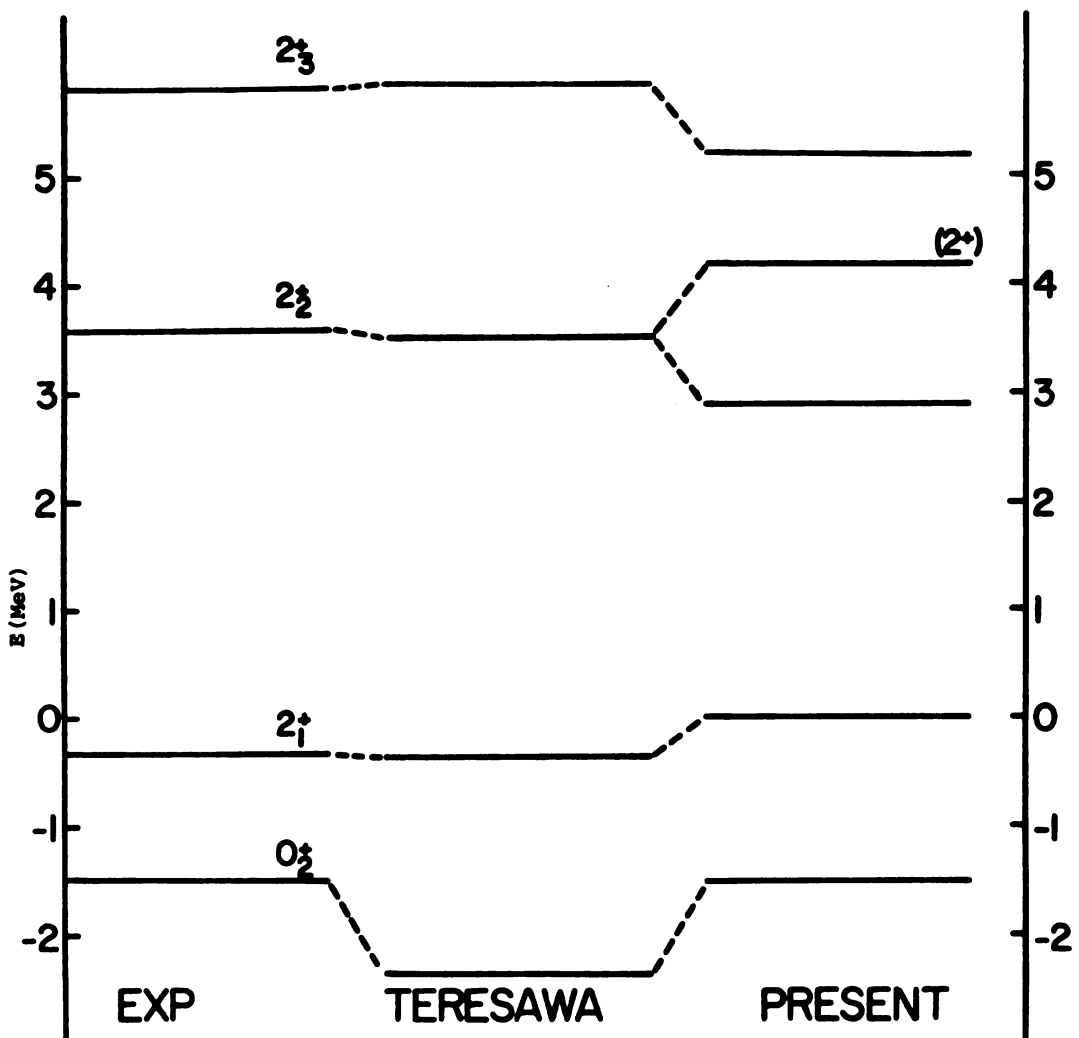


FIG.1.--Spectra from experiment, TTM's calculation and present calculation using TTM's potential.

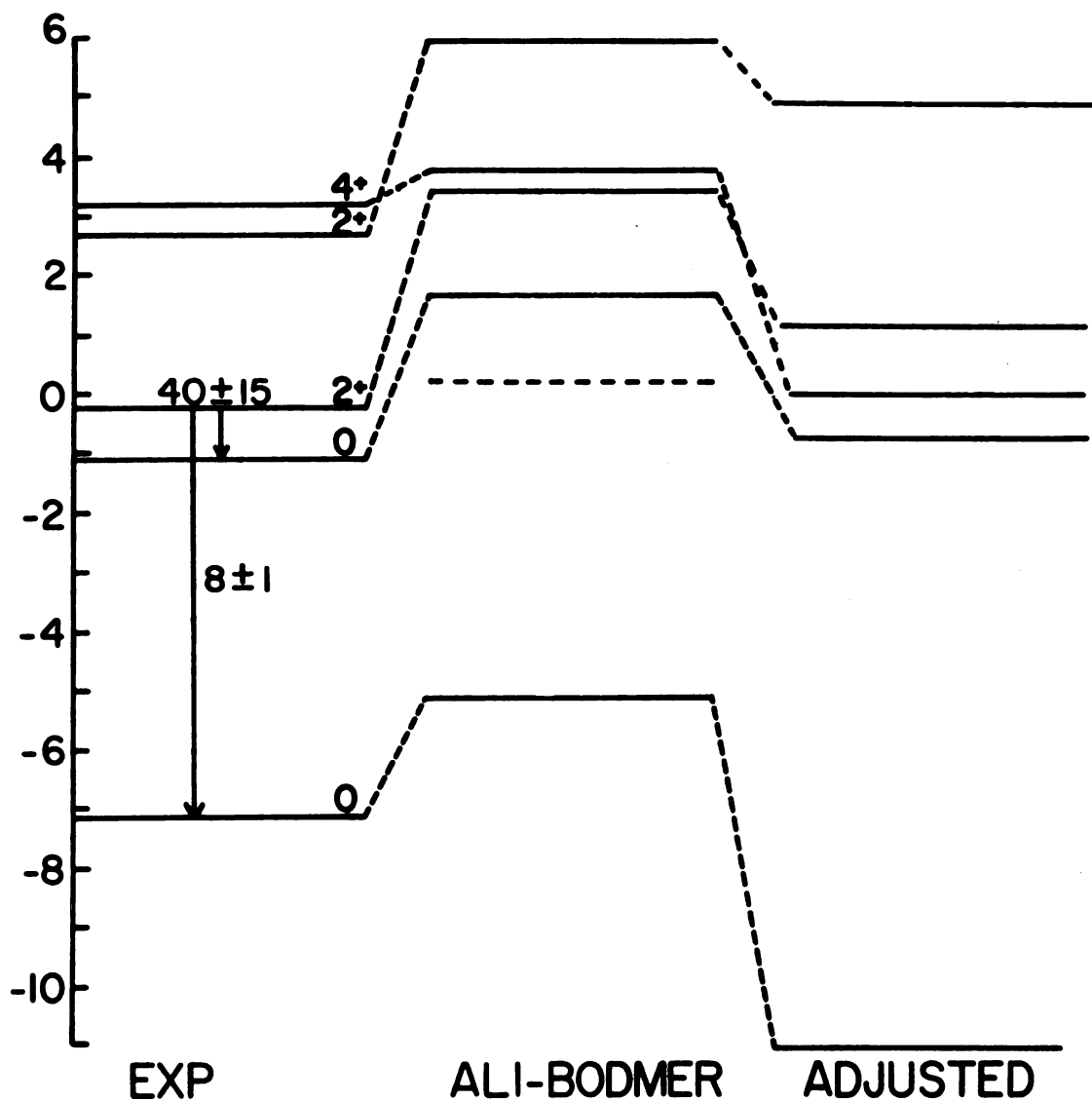


FIG.2.--Spectra from experiment, calculation using Ali and Bodmer potential and calculation using adjusted Ali and Bodmer potential.

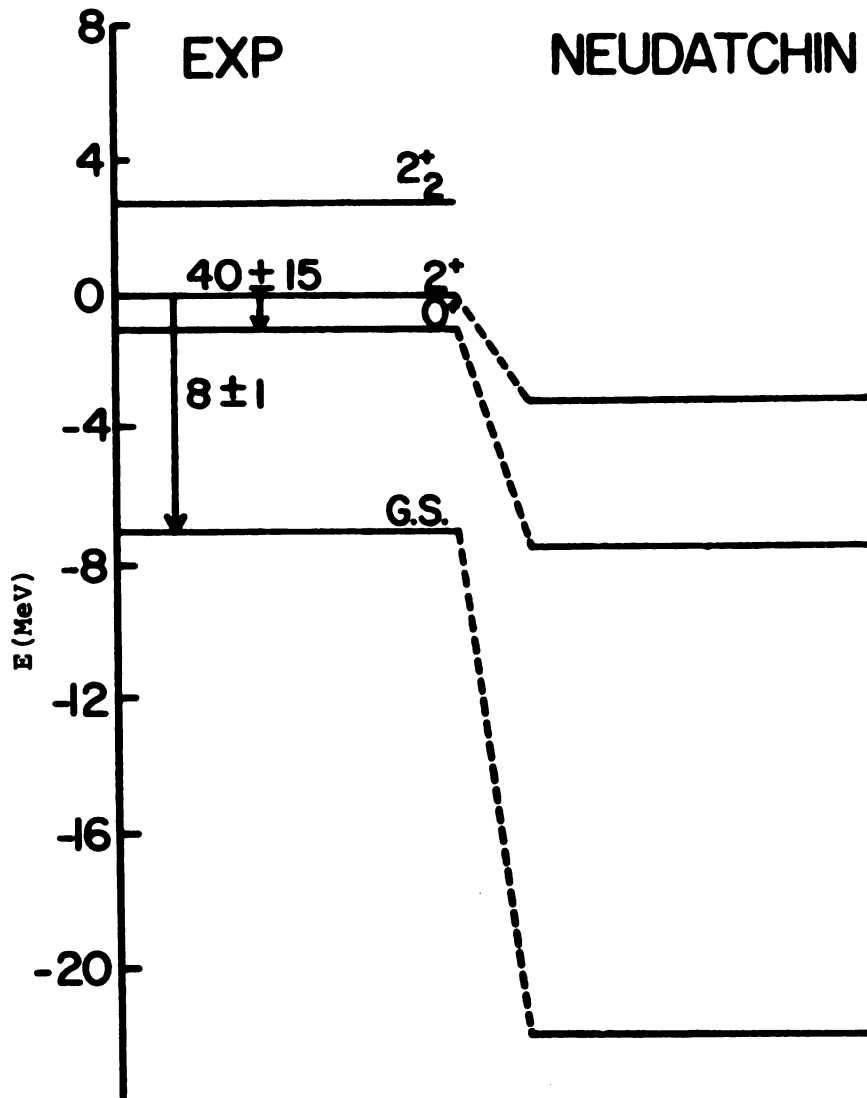


FIG.3.--Spectra from experiment and calculation using Neudatchin potential.

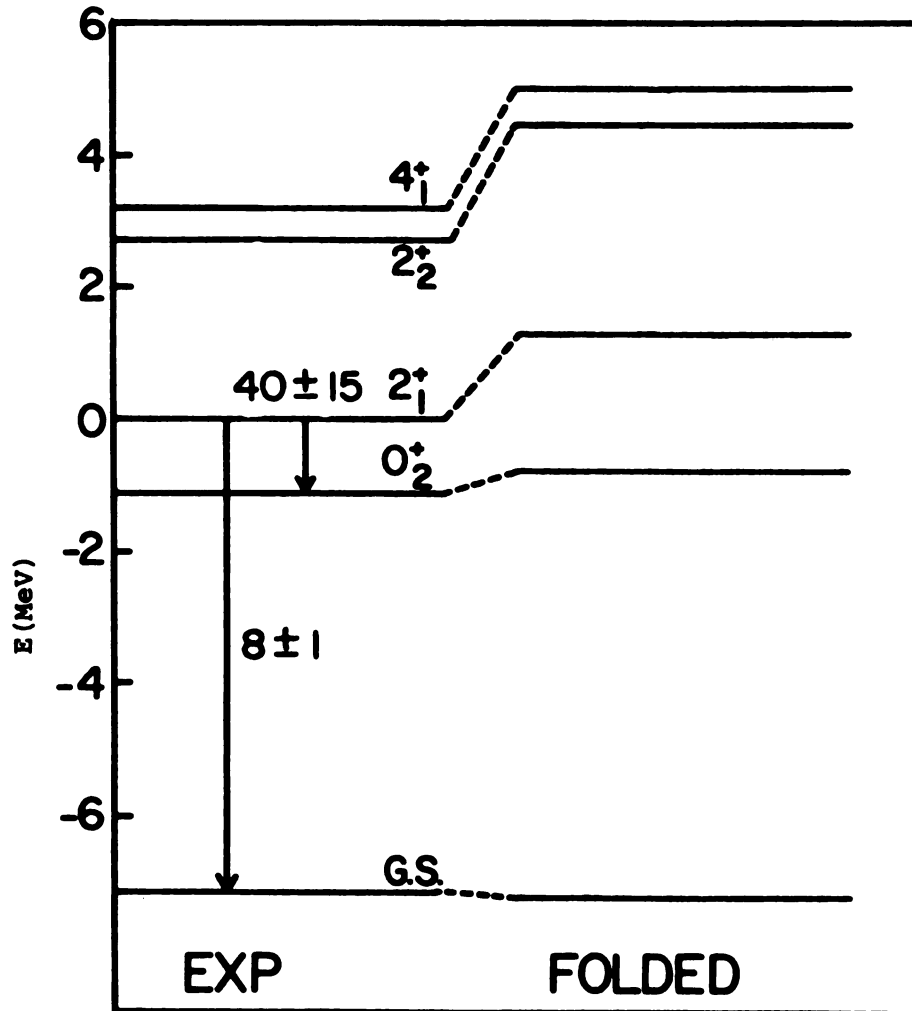


FIG. 4.--Spectra from experiment and calculation using adjusted folded potential.

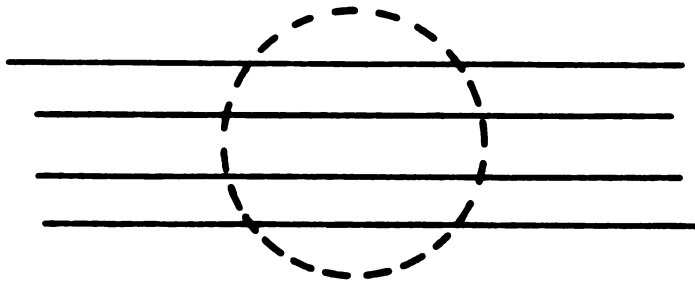
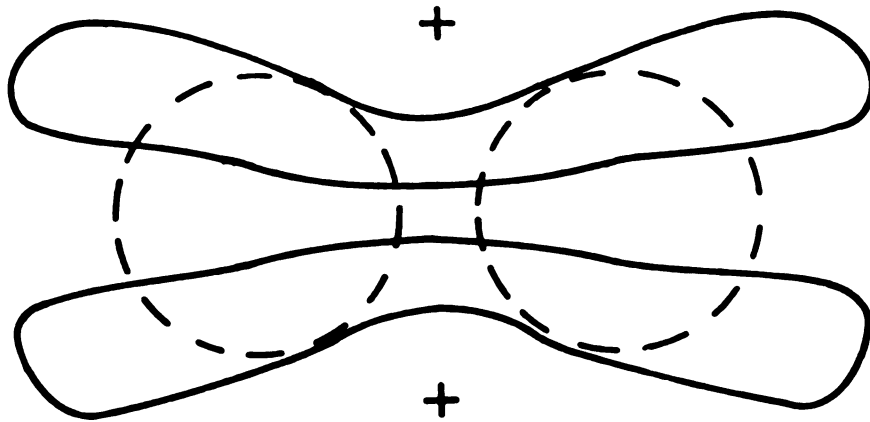


FIG.5. --Nodes of $\alpha+\alpha$ system in ground state, dashed line represents the region where the two α particles overlap.



⁺The place where the wave function most concentrates on.

FIG. 6.--Nodes of the $\alpha + {}^{12}\text{C}$ in ground state for Neudatchin potential, the dashed lines represent the locations of the α particles in the ${}^{12}\text{C}$ core

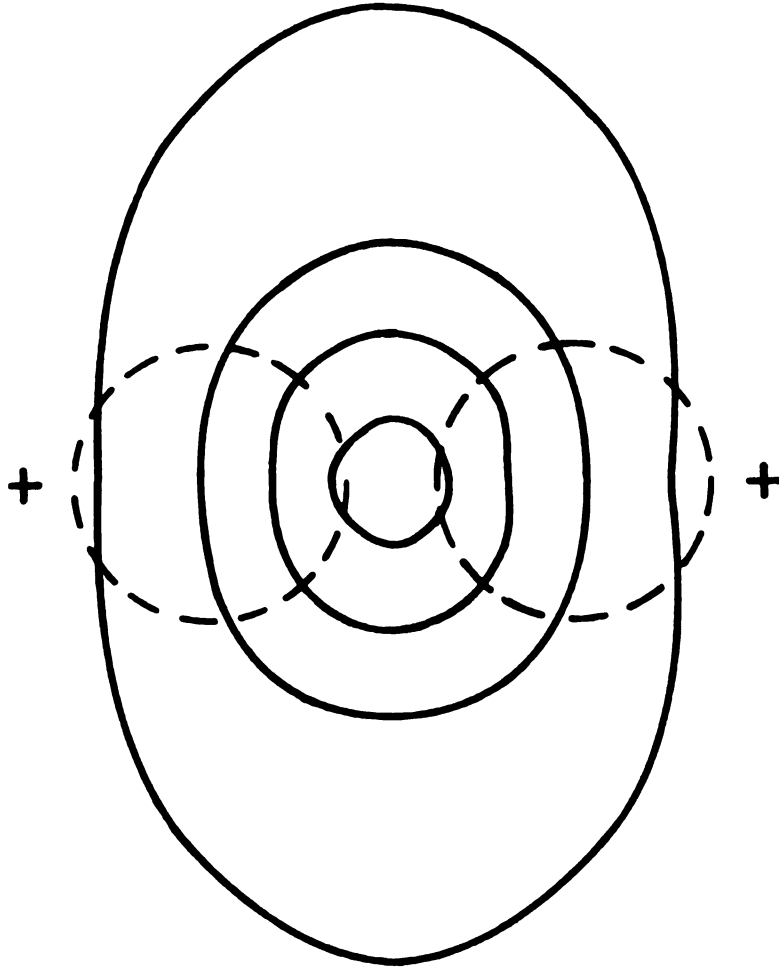


FIG.7.--Nodes of the $\alpha + {}^{12}\text{C}$ in 0_2^+ state for Neudatchin potential.

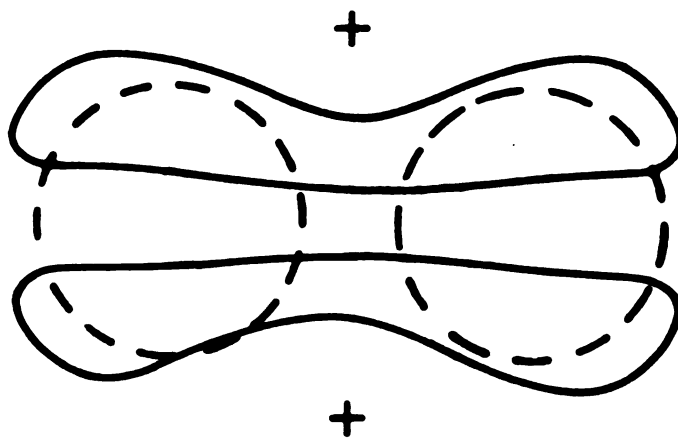


FIG.8.--Nodes of the $\alpha + {}^{12}\text{C}$ in ground state for the adjusted folded potential.

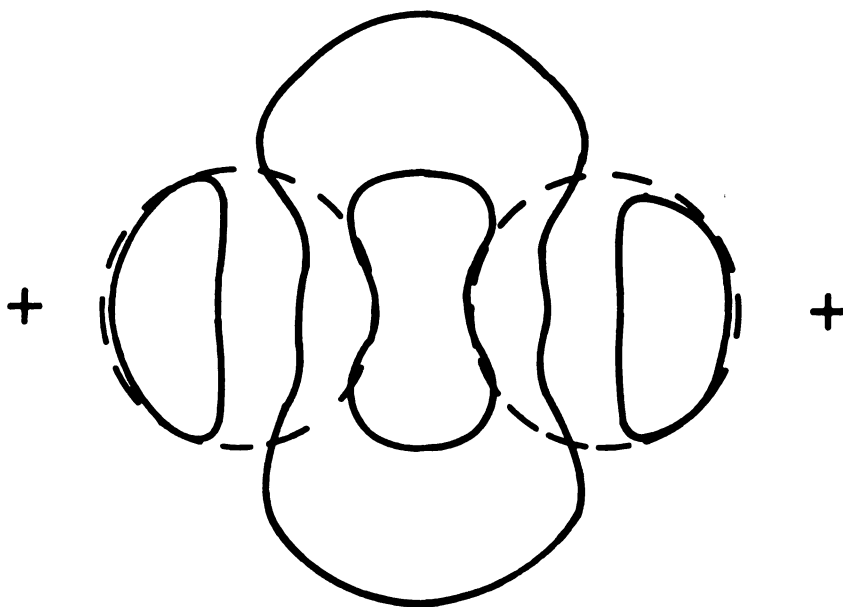


FIG.9.--Nodes of the $\alpha + {}^{12}\text{C}$ in 0_2^+ state for the adjusted folded potential.

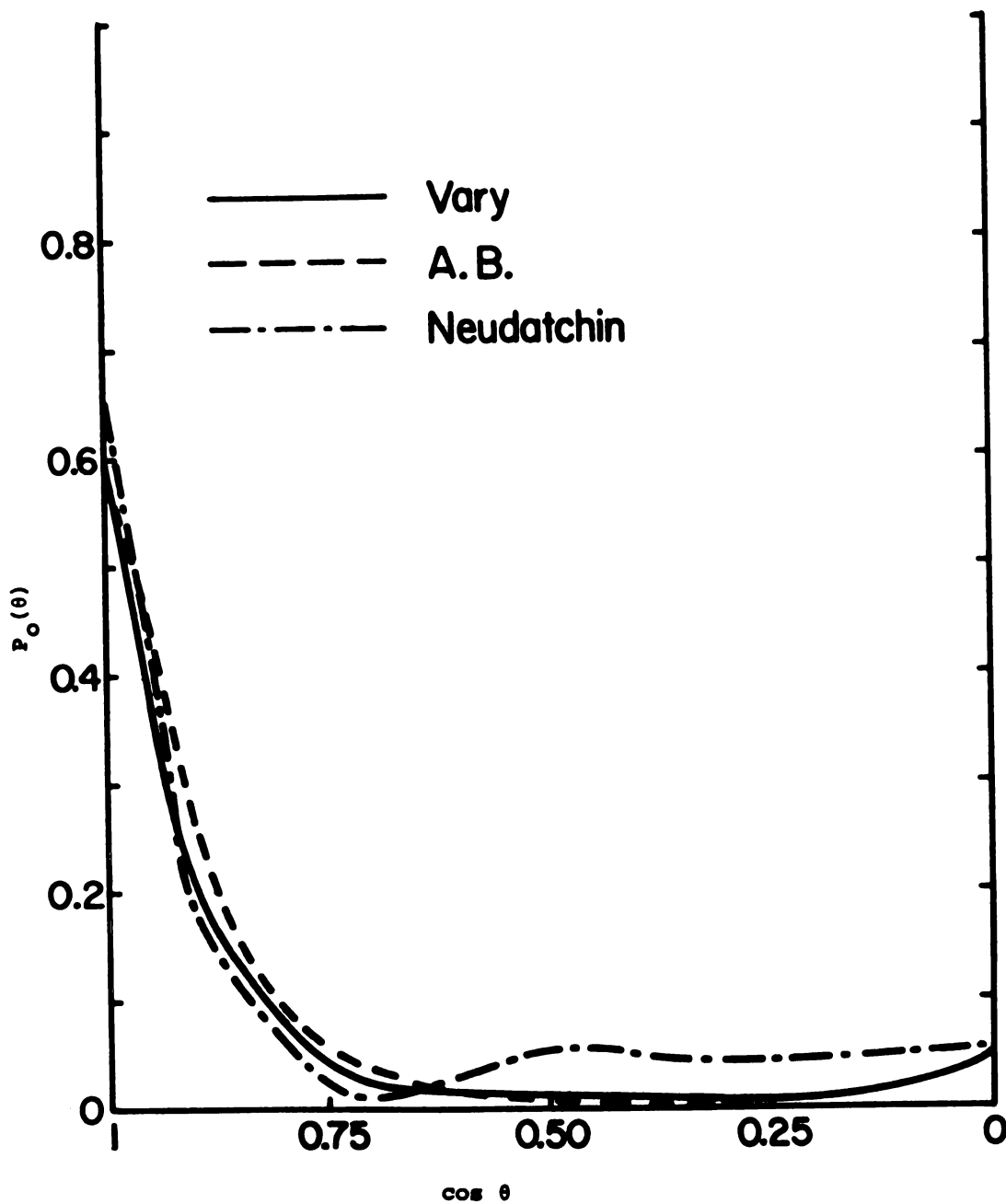


FIG.10.--The plots of $P_0(\theta)$ for ground state versus $\cos(\theta)$ for different potentials.

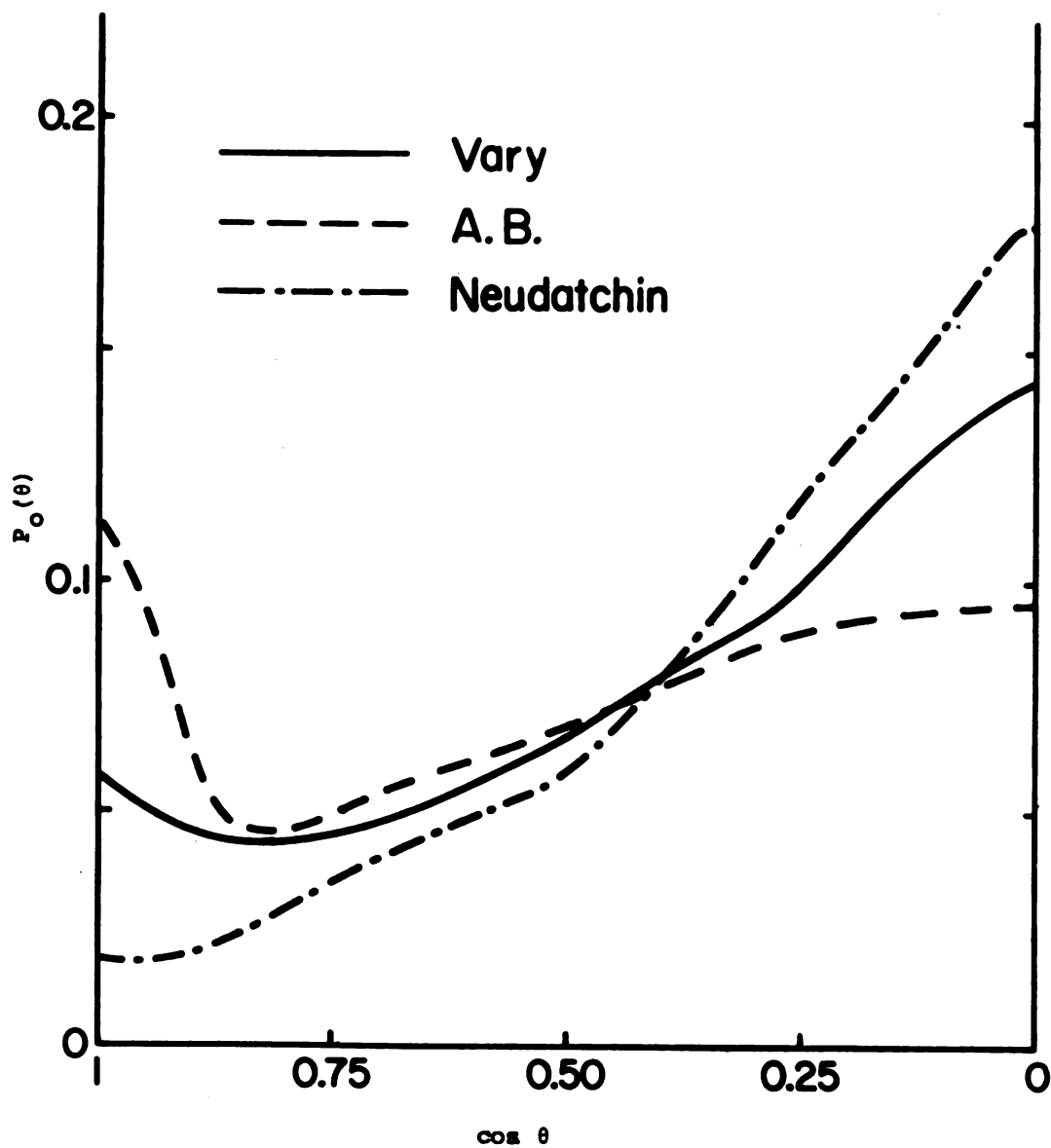


FIG.11.--The plots of $P_0(\theta)$ for 0_2^+ state versus $\cos(\theta)$ for different potentials.

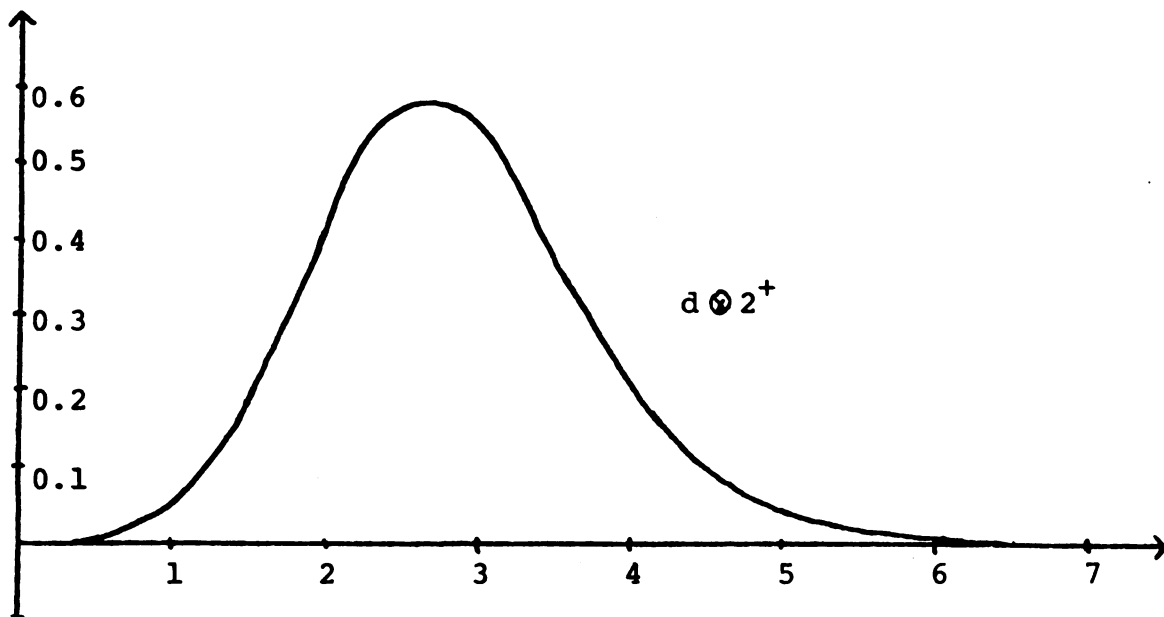
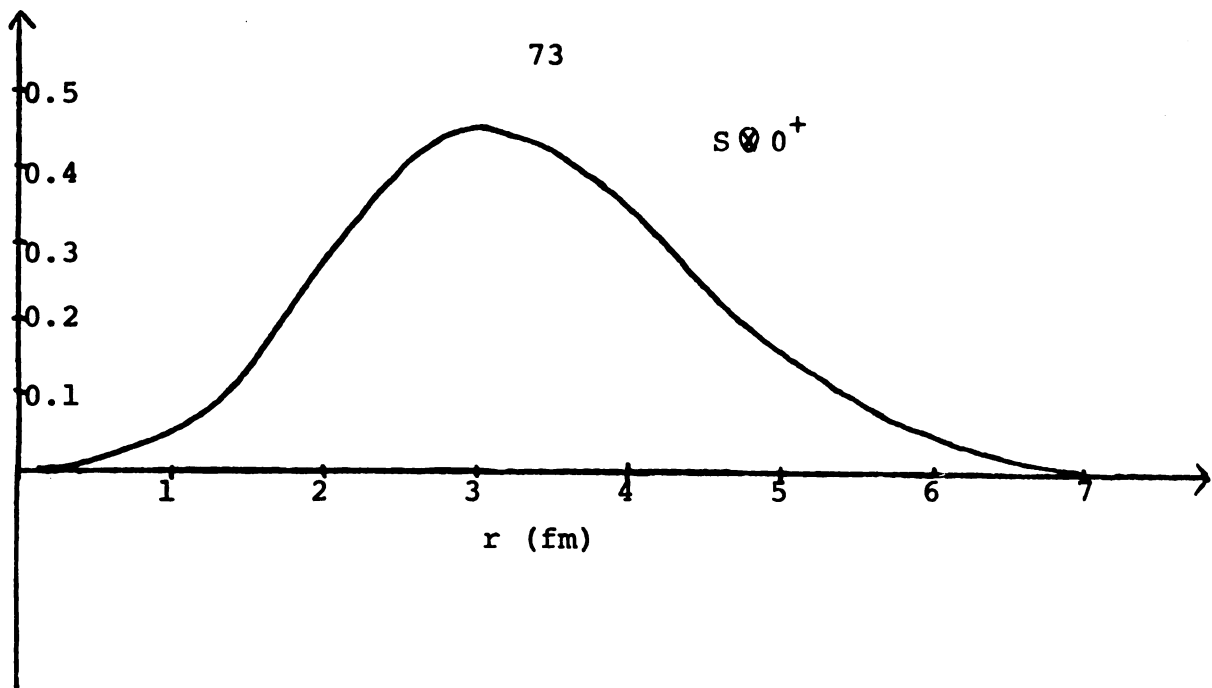


FIG.12. Ground state wave function for Ali and Bodmer potential.

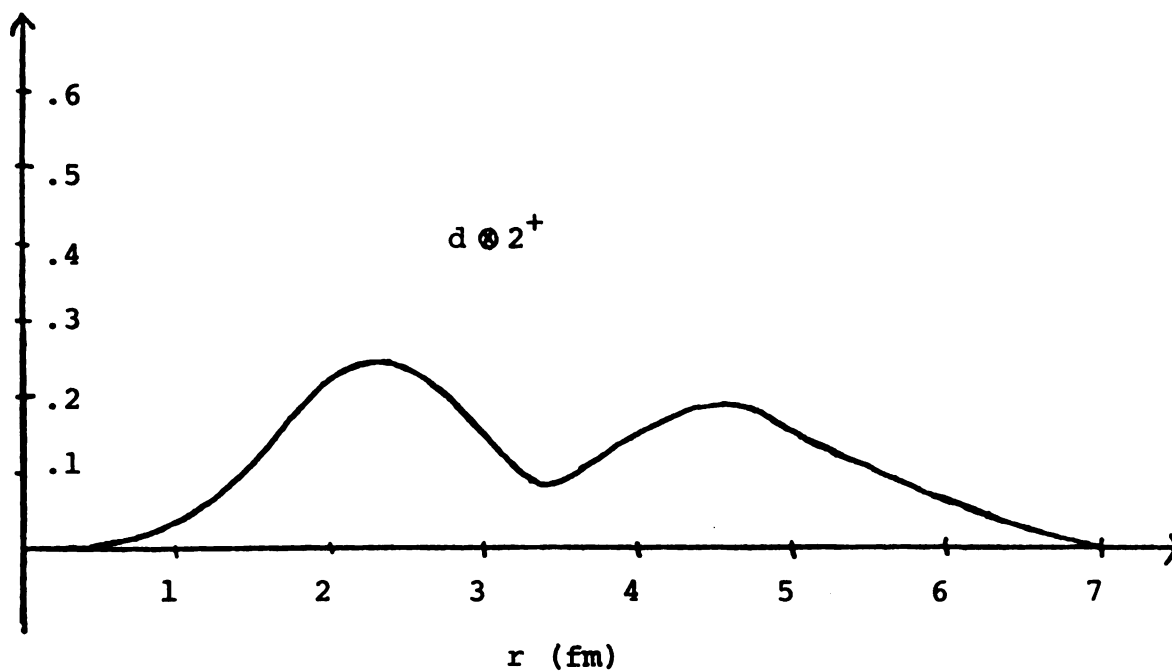
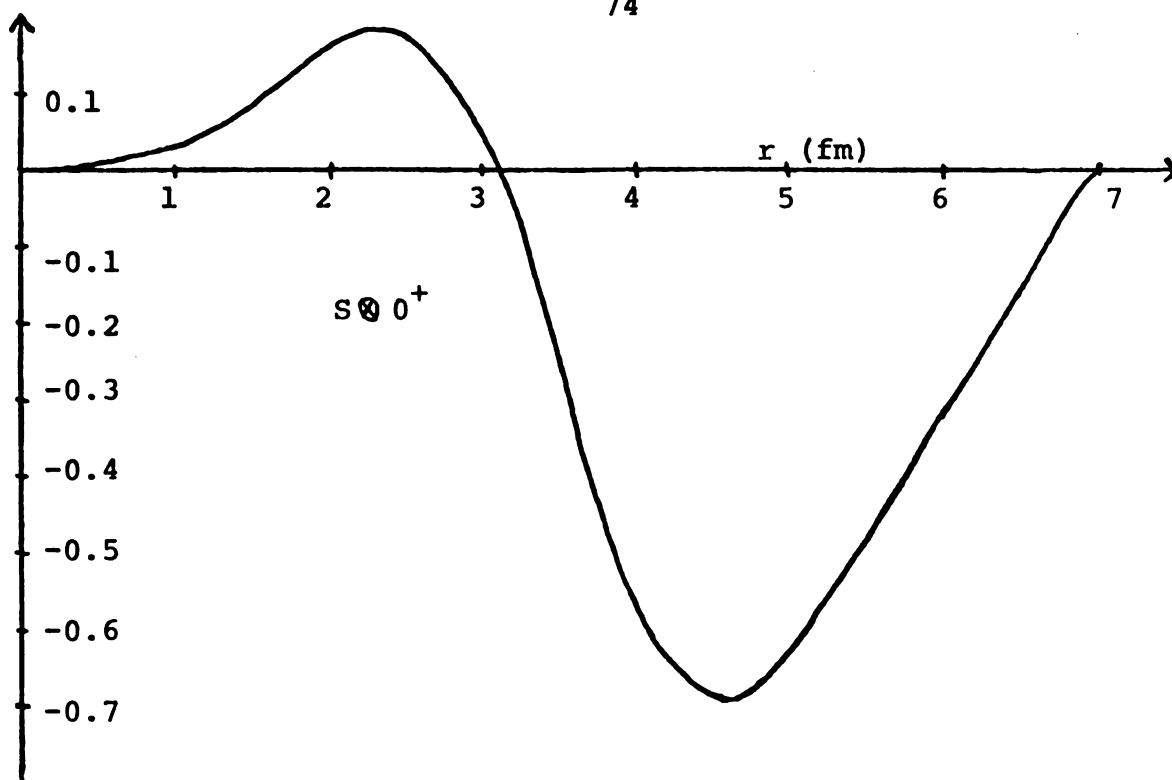


FIG.13.-- 0_2^+ state wave function for Ali and Bodmer potential.

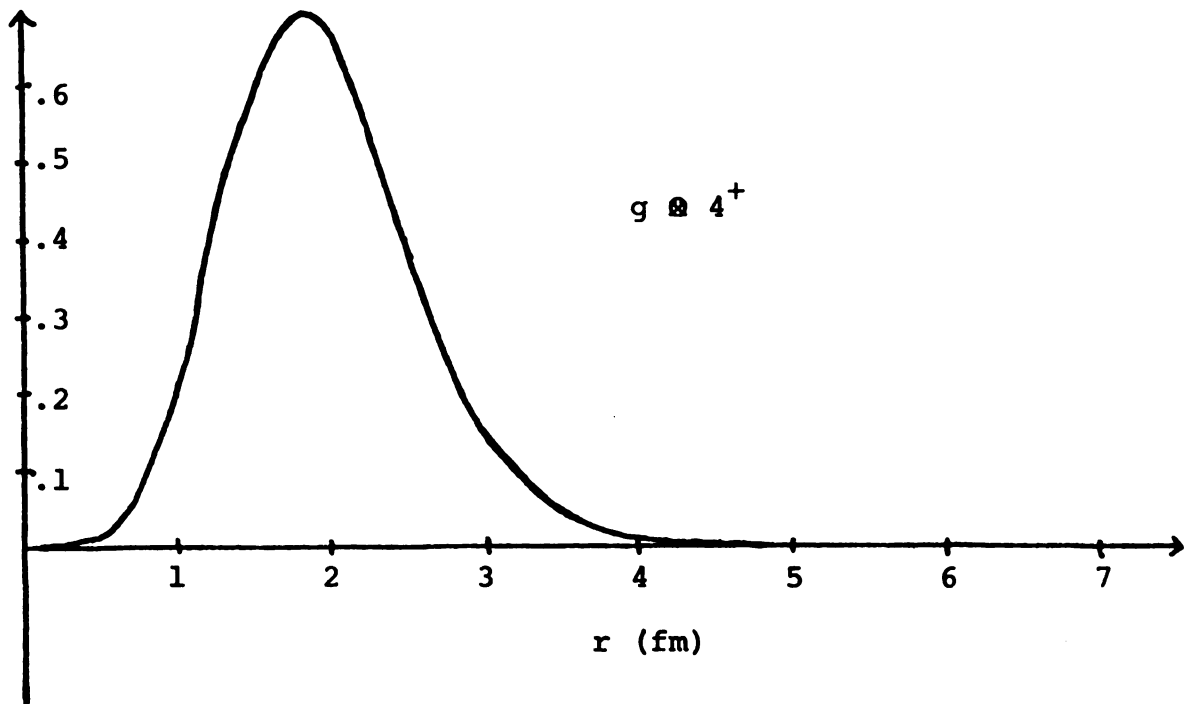
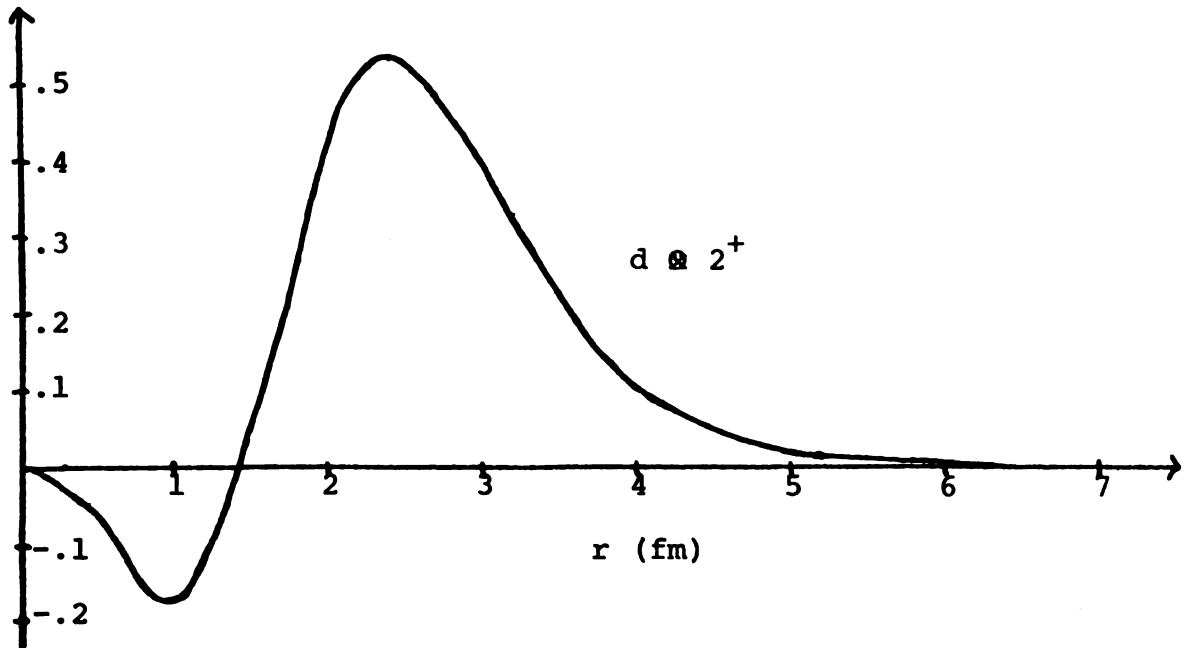


FIG.14.--Ground state wave function for adjusted Folded potential.

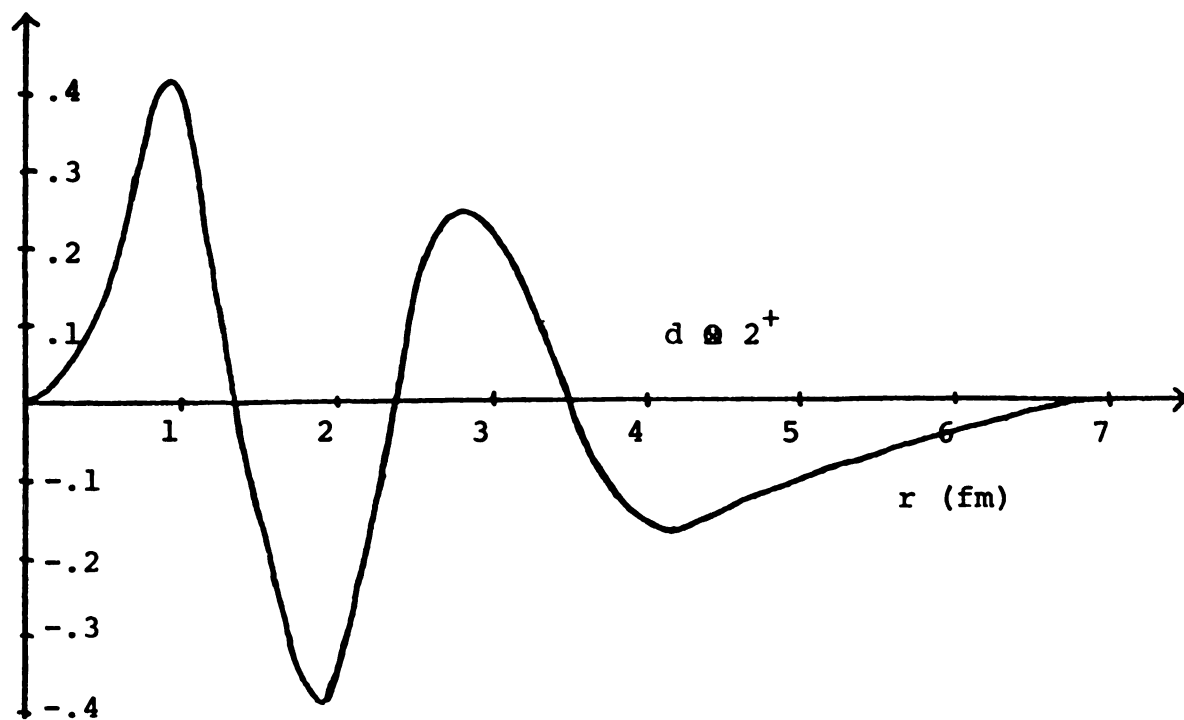
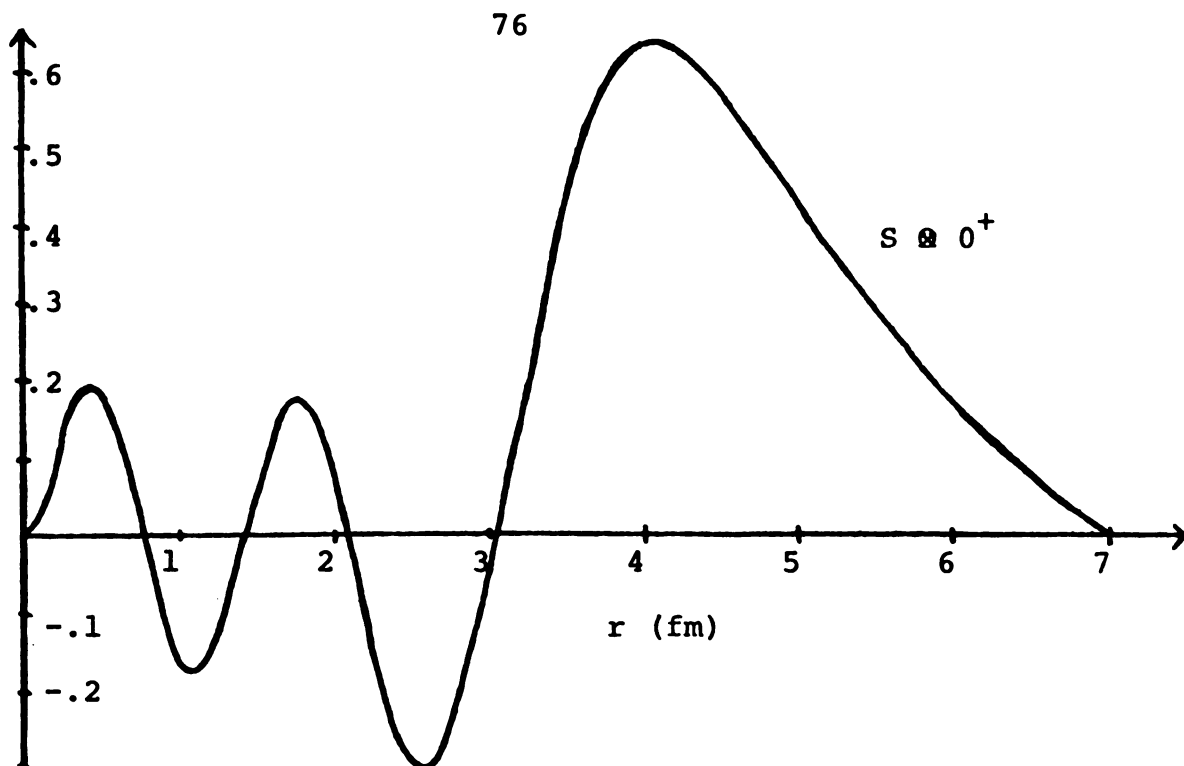


FIG. 15.-- 0_2^+ state wave function for adjusted Folded potential.

MICHIGAN STATE UNIVERSITY LIBRARIES



3 1293 03177 8933